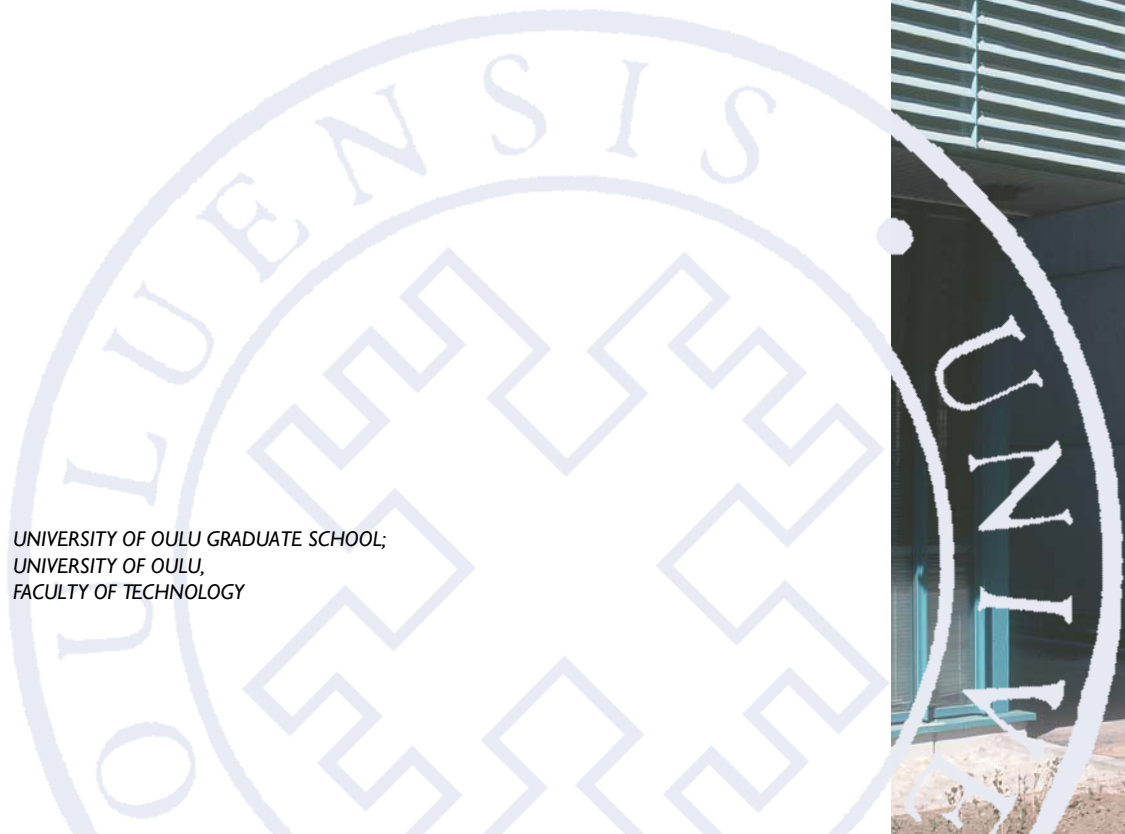


Ehsan Hassani Nezhad Gashti

THERMO-MECHANICAL
BEHAVIOUR OF GROUND-
SOURCE THERMO-ACTIVE
STRUCTURES

UNIVERSITY OF OULU GRADUATE SCHOOL;
UNIVERSITY OF OULU,
FACULTY OF TECHNOLOGY



ACTA UNIVERSITATIS OULUENSIS
C Technica 591

EHSAN HASSANI NEZHAD GASHTI

**THERMO-MECHANICAL BEHAVIOUR
OF GROUND-SOURCE THERMO-
ACTIVE STRUCTURES**

Academic dissertation to be presented with the assent of the Doctoral Training Committee of Technology and Natural Sciences of the University of Oulu for public defence in Auditorium IT116, Linnanmaa, on 9 December 2016, at 12 noon

UNIVERSITY OF OULU, OULU 2016

Copyright © 2016
Acta Univ. Oul. C 591, 2016

Supervised by
Professor Kauko Kujala
Professor Mikko Malaska

Reviewed by
Professor Hussein Mroueh
Professor Tim Länsivaara

Opponent
Professor Ilmo Kukkonen

ISBN 978-952-62-1405-4 (Paperback)
ISBN 978-952-62-1406-1 (PDF)

ISSN 0355-3213 (Printed)
ISSN 1796-2226 (Online)

Cover Design
Raimo Ahonen

JUVENES PRINT
TAMPERE 2016

Hassani Nezhad Gashti, Ehsan, Thermo-mechanical behaviour of ground-source thermo-active structures.

University of Oulu Graduate School; University of Oulu, Faculty of Technology

Acta Univ. Oul. C 591, 2016

University of Oulu, P.O. Box 8000, FI-90014 University of Oulu, Finland

Abstract

High energy prices and new environmental policies have made geothermal energy increasingly popular. The EU, including Finland, aims to increase the use of renewable energy resources and reduce carbon emissions. Geothermal energy pile foundations, so-called energy piles, are considered a viable alternative technology for producing energy instead of traditional methods. Geothermal heat pump systems are economically efficient and renewable environmentally friendly energy production systems in which the ground acts as a heat source in winter and as a heat sink in summer.

Energy piles are economical systems, as they act as dual-purpose structures in energy production and load transfer from buildings to the ground, avoiding extra expenses in ground boring solely for energy production. However, use of ground heat exchangers (GHE) for energy production in energy piles can result in temperature variations in the pile shaft and surrounding soil, in turn affecting the thermo-mechanical behaviour of pile shaft and soil in both structural and geotechnical terms. Despite large numbers of energy piles being installed, there is still a lack of reliable information and experience about the thermo-mechanical behaviour of these structures and their energy efficiency in cold climates.

This thesis investigated the efficiency performance of energy pile foundations and their productivity in cold climates by considering different groundwater flow effects and short-term imbalanced seasonal thermal loadings. The structural and geotechnical bearing capacity of different types of energy piles fitted with GHEs were also evaluated, using numerical models, and the possibility of collapse due to use of thermal systems was examined.

Use of the model to compare the performance of different GHEs in terms of their efficiency revealed that at a particular fluid flow rate, double U-tube systems had greater productivity than other systems tested. The results also indicated that using energy piles under medium groundwater flow can improve the productivity of systems by around 20% compared with saturated conditions with no groundwater flow. It was also concluded that in a design context, the structural bearing capacity of piles needs to be reduced due to the additional thermal stresses induced by heating/cooling pile operations.

Keywords: energy efficiency, energy piles, geotechnical resistance, structural behaviour, thermo-active infrastructures, thermo-mechanical behaviour

Hassani Nezhad Gashti, Ehsan, Maaperäisten termo-aktiivisten rakenteiden termomekaaninen käyttäytyminen.

Oulun yliopiston tutkijakoulu; Oulun yliopisto, Teknillinen tiedekunta

Acta Univ. Oul. C 591, 2016

Oulun yliopisto, PL 8000, 90014 Oulun yliopisto

Tiivistelmä

Kasvaneet energiakustannukset ja kiristyneet ympäristösäädökset ovat lisänneet geotermisten energiaratkaisujen suosiota. EU, mukaan lukien Suomi, on asettanut tavoitteekseen lisätä uusiutuvien energialähteiden käyttöä ja vähentää hiilidioksidipäästöjä. Geotermistä energiaa hyödyntävä paaluperustukset, niin kutsutut energiapaalut, tarjoavat uudenlaisen teknologian vähäpäästöisen energian tuottamiseen. Geotermiset lämpöpumppujärjestelmät, maalämpöpumput, ovat taloudellisia ja ympäristöystävällisiä energiantuotantomenetelmiä, jotka talviaikaan siirtävät maaperään varastoitunutta energiaa rakennuksen lämmittämiseen ja vastaavasti jäädyttävät rakennusta kesällä siirtämällä lämpöä maaperään.

Energiapaalujen taloudellisuus syntyy siitä, että ne pystyvät palvelemaan rakennusta kahdessa roolissa. Ne ovat osa rakennuksen energiajärjestelmää ja toimivat samalla myös kantavana rakenteena, joka siirtää rakennuksen kuormia perustuksilta maaperään. Lämpöpumppujärjestelmän kytkeminen paaluihin voi johtaa lämpötilan vaihteluun paaluissa sekä niitä ympäröivässä maaperässä, mikä puolestaan vaikuttaa paalujen ja maaperän lämpömekaanisiin, rakenteellisiin sekä geoteknisiin ominaisuuksiin. Vaikka energiapaaluja on asennettu jo paljon, ei paalujen lämpömekaanisesta käyttäytymisestä tai energiatehokkuudesta kylmien ilmastojen alueilla ole vielä paljoa tutkittua tietoa.

Tässä väitöstutkimuksessa selvitettiin numeerisesti energiapaalujen rakennuspaikan pohjaolosuhteista riippuvaa tuottopotentiaalia Skandinaavisissa olosuhteissa ja ilmastossa. Tarkastellut kohdistuivat erityisesti pohjavesivirtauksen sekä vuodenaikojen ja ilman lämpötilan vaihtelun vaikutuksiin. Tutkimuksessa arvioitiin myös paalujen lämpötilan vaihtelujen vaikutuksia paalujen geoteknisiin ja rakenteellisiin ominaisuuksiin sekä kestävyys.

Numeeristen simulaatiotulosten perusteella betonipaaluun asennetun U-putkirakenteen avulla saavutetaan paras tuottopotentiaali. Tulokset osoittivat, että kohtalainen pohjaveden virtaus parantaa systeemin tuottoa noin 20 % verrattuna tilanteeseen, jossa vedellä kyllästetyssä maassa ei tapahdu pohjaveden virtausta. Analyysitulokset osoittavat myös, että paalujen lämpötilavaihteluista aiheutuvat lisäjännitykset vähentävät paalujen kantokykyä, mikä tulee ottaa huomioon paalujen mitoituksessa.

Asiasanat: energiapaalut, energiatehokkuus, geotekninen kestävyys, lämpö-aktiiviset infrastruktuurit, rakenteellinen käyttäytyminen, termomekaaninen käyttäytyminen

To my loved ones

Acknowledgements

I would like to express my deepest gratitude to my supervisors Prof. Kauko Kujala and Prof. Mikko Malaska for their supportive comments, advices and encouragements, which enabled me to perform my research with higher motivation in their field of expertise. I would like to thank Prof. Björn Klöve for his constant support during my research, which always helped me to get through the hard stages of my work and made the difficulties of this long plan smoother to me. Thanks to my pre-examiners Prof. Hussein Mroueh and Prof. Tim Länsivaara for their valuable contribution in finalising this thesis; to my opponent Prof. Ilmo Kukkonen for accepting this task; and also to Dr. Mary McAfee for her language revision of the thesis manuscript. I would like to gratefully acknowledge the funding awarded for this project mainly by Koneen Säätiö of Finland since January 2013.

Warm thanks to my dear colleagues and friends for their help, smiles and supportive words, which encouraged me to in my research. My friends Shahram and Ali, I owe you very special thanks for your never-ending supports and helps, which encouraged me to continue during the hardest times of this task. Many thanks also to Veli-Matti Uotinen for his worthwhile contributions in publication of our joint paper.

I would like to express my warmest and deepest thanks to my parents for keeping me going onward with this work and supporting me in every stage of my life, which was a great help and motivation in travel along this hard path. I would also like to thank my friends and all others who supported me in this study.

Oulu, December 2016

Ehsan Hassani Nezhad Gashti

Abbreviations

GHE	Ground heat exchanger
GSHP	Ground source heat pump
PE	Polyethylene
COP	Coefficient of performance

Original publications

This thesis is based on the following publications, which are referred throughout the text by their Roman numerals:

- I Hassani Nezhad Gashti E, Uotinen V-M, Kujala K, (2014) Numerical modelling of thermal regimes in steel energy pile foundations: A case study. *Energy and Buildings* 69: 165-174. DOI: 10.1016/j.enbuild.2013.10.028.
- II Hassani Nezhad Gashti E, Malaska M, Kujala K, (2014) Evaluation of thermo-mechanical behaviour of composite energy piles during heating/cooling operations. *Engineering Structures* 75: 363-373. DOI: 10.1016/j.engstruct.2014.06.018.
- III Hassani Nezhad Gashti E, Malaska M, Kujala K, (2015) Analysis of thermo-active pile structures and their performance under groundwater flow conditions. *Energy and Buildings* 105: 1-8. DOI: 10.1016/j.enbuild.2015.07.026.

The author's contribution to the publications listed was as follows:

- I Designed the study, developed the model, conducted the data analysis and wrote the paper. Veli-Matti Uotinen gathered data for validation of model. Kauko Kujala commented on the manuscript.
- II Designed the study, developed the model, conducted the analysis and wrote the paper. Mikko Malaska and Kauko Kujala commented on the manuscript.
- III Designed the study, developed the model, conducted the analysis and wrote the paper. Mikko Malaska and Kauko Kujala commented on the manuscript.

Contents

Abstract	
Tiivistelmä	
Acknowledgements	9
Abbreviations	11
Original publications	13
Contents	15
1 Introduction	17
1.1 Energy piles.....	18
1.2 Heat transfer and energy efficiency.....	19
1.3 Thermo-mechanical behaviour of energy piles.....	20
1.4 Objectives of the thesis and key assumptions.....	23
2 Case studies	25
2.1 Summary of test pilot site.....	25
3 Methodology	27
3.1 Thermal analysis.....	27
3.1.1 Model specifications.....	27
3.2 Mechanical behaviour.....	32
3.2.1 Theoretical background and governing equations.....	32
3.2.2 Numerical modelling.....	35
3.3 Groundwater flow effects.....	42
3.3.1 Equations used in the model.....	42
3.3.2 Model description.....	43
4 Results and discussion	47
4.1 Thermal analysis.....	47
4.1.1 Heat exchange rates of GHEs in heating and cooling operations.....	48
4.1.2 Thermal regime in pile shaft.....	52
4.2 Mechanical analysis.....	53
4.2.1 Temperature-induced stresses.....	55
4.2.2 Temperature-induced displacements.....	60
4.2.3 Mobilised shaft friction.....	63
4.3 Energy piles under groundwater flow effects.....	65
4.3.1 Energy production.....	65
4.3.2 Thermo-mechanical behaviour of the pile.....	68
5 Conclusions and suggestions for future studies	73

List of references	79
Original publications	83

1 Introduction

With high energy prices and new environmental policies, the use of geothermal energy has become increasingly popular. The EU, including Finland, aims to increase the use of renewable energy resources, become more self-sufficient and reduce carbon emissions [1-3].

Geothermal heat pump systems are considered an economically efficient and renewable environmentally friendly method for heating and cooling building interiors [4]. They are becoming increasingly popular due to the significant developments made in the technology in recent years [5-9]. The system is based on absorption of heat from the ground during winter (as heat source) and injection of heat into the ground during summer (as heat sink) (Fig. 1).

Heat transfer in surrounding soil and the ground heat exchanger (GHE) can influence the productivity of the system by affecting the potential of the ground to act as a heat source/sink for heat extraction/injection. When the difference between the surrounding soil temperature and the heat carrier fluid inside the tube is higher, more energy production can be expected. In the long term, the geothermal potential of the ground decreases when a geothermal heat pump system is in operation, which can affect the productivity of the system. Consequently, selection of a suitable location for these systems is highly important, as compensating for the primary costs of system installation requires feasible long-term performance of geothermal heat pump systems.

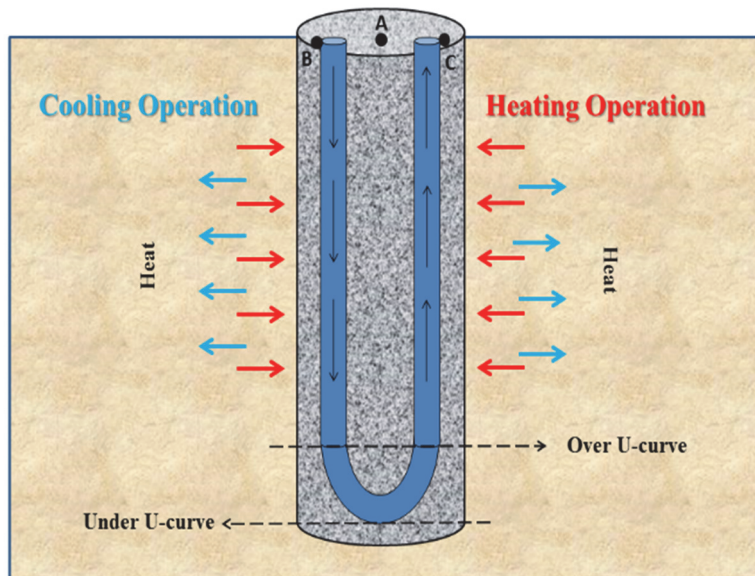


Fig. 1. Heating/cooling operations of energy piles by absorbing/injecting heat from/to the ground during winter/summer mode (Paper I, reprinted with permission from Journal Energy and Buildings).

1.1 Energy piles

Pile foundations equipped with GHEs, so-called energy piles, are considered viable alternative technology for producing energy instead of conventional systems. This relatively new technology is a suitable method to reduce carbon dioxide emissions during the production of energy for heating/cooling buildings, as the extra cost of soil drilling to install the GHEs is avoided. This heat exchanger system also benefits from the higher thermal conductivity of a pile shaft made of concrete and steel than a borehole filled with grout, which can increase energy transfer between the system and the ground. Statistics show that there is increasing interest in using this relatively new technology world-wide (around 80 countries around the world have been using geothermal energy for different heating and cooling objectives since 2000) [10]. Numerical and analytical studies have been carried out to examine the effects of groundwater flows on the performance of deep GHEs [11-12], but very

few have included energy pile foundations influenced by groundwater flow and the imbalanced seasonal thermal loadings in cold climates.

In view of the two cooling/heating thermal regimes generated at the pile and in surrounding soil, two different mechanisms of pile mechanical behaviour can be expected; pile shaft contraction in winter mode, caused by colder fluid entering the tubes, and pile shaft expansion in summer mode, induced by hotter fluid. The use of energy pile foundations can be of great importance if the bearing capacity of piles in both structural and geotechnical perspectives remains within the permitted ranges set by building codes. Despite the large number of energy pile installations in existence [13-16], few previous studies have examined the thermo-mechanical behaviour of piles, in particular in different pile-soil interface conditions.

1.2 Heat transfer and energy efficiency

A classic method in modelling the thermal regimes around GHEs is that presented by Carslaw and Jaeger [17], which is based on cylindrical heat source theory, extended for an infinite pipe length surrounded by a homogeneous soil. This method has been utilised by a number of researchers in numerical analyses of GHE performance [18-20]. It has also been used in an extended form in some analytical models, e.g. those presented by Ochifuji and Kim [21] and Bernier [22]. However, all these models are based on constant cylindrical shape of the GHE by assuming constant diameter at depth. Hence, they are unable to analyse the effect of a U-tube shaped heat exchanger inside the piles, which could hamper accurate prediction of GHE performance and thermal regimes generated around the system.

With the appearance of software based on finite element theory, many analyses of complex mathematical problems have been conducted. In recent years, a number of numerical models have been applied to simulate the performance of GSHP systems based on this theory and the data obtained have been compared against experimental results [23-27]. For example, Nam *et al.* [28] used a numerical finite element model to calculate heat exchange rate in a GSHP system in China. In that model, heat transfer in surrounding domains was modelled based on GHE performance in concrete piles with non-steady state analysis. The numerical results were then compared against experimental values, and good agreement was found. Much experimental work has concentrated on analysis of GSHP system performance and evaluation of productivity in different climates (e.g. examination of coefficient of performance, COP). However, there are far fewer numerically validated studies concentrating on the thermal regimes generated in the energy pile

shaft, which reflects the actual operation of the system in three-dimensional (3D) real scale based on the exact shape of the U-tubes inside the piles.

In this thesis, the thermal operation of common energy piles utilised in Finland was analysed numerically based on real conditions of system performance in heating and cooling operations in the Finnish climate. For the analysis, a 3D model based on finite element theory was defined in the Comsol Multiphysics package and the performance of the system with and without groundwater flow conditions was analysed. The model was operated in real scale of the pile and surrounding environment and reflected the exact shape of the polyethylene (PE) U-tubes in the system. The model simulated heat transfer by coupling forced convection and conduction processes from the heat-carrier fluid inside the pipes into the ambient materials. Model results were then compared with experimental values measured in a pilot test conducted at Hämeenlinna in southern Finland to validate the numerical model. The GHE power for some different U-tube shapes was also determined and the values compared, in order to identify the most efficient system. Temperature variations in vertical and horizontal axes along the pile length in a single U-tube system were determined in different heating and cooling operations and the results were compared with the constant temperature assumption along the entire pile length. The results obtained from these thermal regime analyses were then used for calculating extra thermal stresses and deformation in energy piles in the next stage of the research, as correct prediction of thermal stresses and deformations in energy piles is impossible unless thermal regimes generated from heat transfer regarding the real operations of GHEs are first accurately taken into consideration. The numerical model developed is sufficiently flexible to be extended for further investigations of thermal regimes in energy piles under various climates and GSHP operations.

1.3 Thermo-mechanical behaviour of energy piles

Heat transfer in energy piles results in thermal fluctuations in the pile shaft, since the heat carrier fluid circulated within the tubes by GSHPs is colder/hotter than the surrounding ground temperature during winter/summer. These heating/cooling operations cause the pile shaft to expand/contract (Fig. 2). This expansion/contraction behaviour of the pile shaft may affect the bearing capacity of the pile as regards geotechnical and structural resistance.

Detailed study of these fluctuations is highly important due to their ability to affect the mechanical behaviour of energy piles by generation of extra stresses and

deformations [13]. Energy piles can have great potential for heating/cooling applications in terms of their long-term performance as regards sustainability, economics and flexibility [29] provided that pile durability (in both mechanical and geotechnical terms) remains in the ranges recommended by reliable building codes.

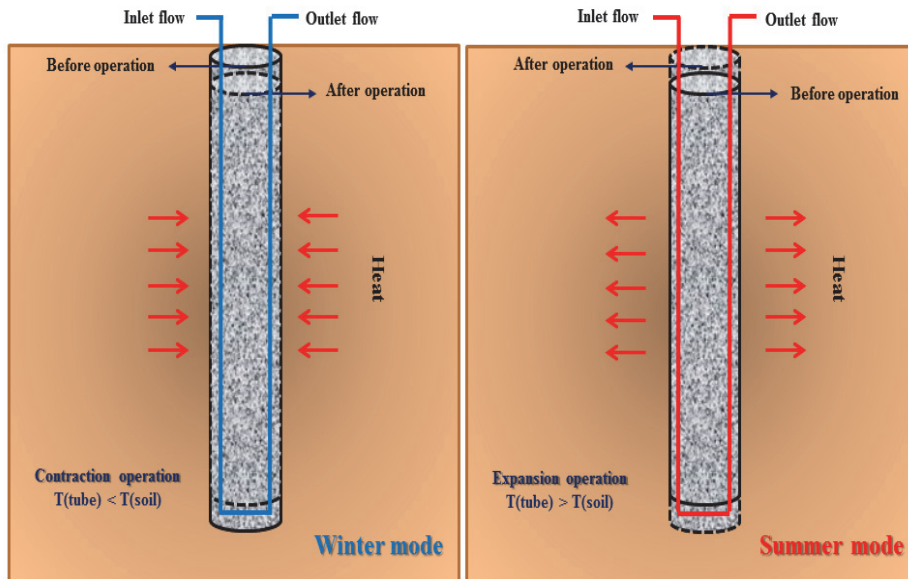


Fig. 2. Thermo-mechanical behaviour of energy pile foundations in different thermal loading conditions (Paper II, reprinted with permission from Journal Engineering Structures).

Prefabricated reinforced concrete driven piles fitted with GHEs are currently the most commonly installed form of energy pile system [30]. Ductile cast iron piles fitted with GHEs have also become more widely used recently, with the aim of reducing the risk of GHE damage to pile installations [30]. During the past decade, energy piles have been used in many large construction projects [13], e.g. Germany (Frankfurt Main Tower; over 112 drilled energy piles) [14], Switzerland (dock at Zürich airport; with 315 energy piles) [15] and Austria (Lainzer tunnel in Vienna; with foundations containing 59 energy piles) [16]. However, despite this large number of installations, there is still a lack of reliable information on the technology. For example, little is known about the thermo-mechanical behaviour of energy piles under different thermal loading conditions, particularly as regards composite energy piles. Suryatriyastuti *et al.* [31] introduced a preliminary numerical model

of a concrete energy pile which simulates pile behaviour using finite element analysis and static thermal loading conditions. That study examined two different sets of conditions at the soil-pile interface, namely perfect contact (without relative movement between soil and pile surface) and sliding contact, and assumed constant temperature along the entire pile length. The results showed that for piles with simply supported ends and with perfect contact between soil and pile, the thermal-induced stresses generated are higher than those with sliding contact. Laloui *et al.* [13] also carried out in situ pile tests and introduced a simple numerical model for energy pile behaviour. The model was tested in a four-storey building under construction at the Swiss Federal Institute, Lausanne, which was built on 97 piles approximately 25 m in length. Those authors concluded that a temperature gradient of 1°C can induce extra vertical forces of 100 kN in energy piles and that the numerical model they developed could satisfactorily predict the thermo-mechanical behaviour of energy piles. However, in both numerical models [13,31], a fairly simple method was used for calculating thermo-mechanical behaviour. The models were unable to analyse the effect of the shape and location of the heat exchanger tubes inside the pile shaft and could therefore have provided incorrect predictions of the thermo-mechanical behaviour of the system.

Despite the large number of energy piles now in use, there have been few studies, numerical studies in particular, on the complex thermo-hydro-mechanical behaviour of these structures. Therefore in this thesis different types of pile foundations were analysed numerically using a 3D model of piles and soil. Data on the exact shape of the U-tubes inside the piles were used in the models and the effects of the tubes on the mechanical behaviour of the structural system were studied. A 3D thermo-hydro-mechanical analysis was carried out using the finite element method and the numerical analysis software Comsol Multiphysics package [32]. The analysis assumed static thermal loading conditions and linear elastic and elasto-plastic material behaviour by soil and pile. The mechanical behaviour of the models was linked with thermal analysis by conduction and forced convection processes. Initial and boundary conditions were taken into account based on information obtained from in situ measurements and the real geometry and thermal loading conditions of the system. The thermo-hydro-mechanical behaviour of piles in heating/cooling operation was analysed with respect to the transient conditions of inlet and outlet temperature of the heat carrier fluid inside the pipes and the ground surface temperature. Experimental data from the Lausanne tests [13] were used for validation of the mechanical behaviour of the model and good correlation between the results was found. Temperature-induced stresses, deformations and the

extra mobilised shaft friction in the pile during expansion/contraction were calculated. The results obtained were compared against the current recommended guidelines for using energy piles. The pile system and soil domains were modelled in real scale (without reduction in system dimensions) and the operating history in service mode was based on Finnish climate conditions.

1.4 Objectives of the thesis and key assumptions

The overall aim of this thesis was to enable accurate prediction of energy pile performance in cold climates, which is of great importance in view of the low capacity of shallow geothermal sources during the cold season and high demand for proper and precise prediction of GHE productivity with respect to high demand for energy in the Nordic area.

It is also important for new models to be able to take account of the exact shape of the GHE tubes (U-tubes) inside the pile shaft and the detailed performance of the GHEs, in order to determine the precise thermo-mechanical behaviour of energy pile systems and prevent possible system collapse in future. Hence, a second aim of this thesis was to provide information and guidelines about the thermo-mechanical behaviour of energy piles and the practical considerations concerning their installation in cold climates, and to produce data that can be used for determination of the load capacity of energy piles, including both the geotechnical and structural aspects (temperature-induced stresses, deformations and the extra mobilised shaft friction in the pile during expansion/contraction).

For the modelling of systems, static thermal loading was assumed in all analyses. The soil was assumed to be homogeneous and for the lowermost horizontal boundary condition of simulation models constant temperature was considered, with variations in temperature assumed to be negligible for system operation. Vertical boundaries were assumed to be adiabatic, as the pile was considered a sample of a group of piles and due to symmetrical affects.

The following major research tasks were formulated for the thesis work:

Research task 1: *To determine whether the efficiency of energy piles is affected in cold climates, how their productivity varies under different groundwater flow conditions and the configuration of the most energy-efficient system.*

These issues were examined in Papers I and III. The main objective of Paper I was to evaluate the energy efficiency of different pipe configurations on the typical types of energy pile foundations in Finland and the productivity of the systems

based on local soil and cold climate. For comparison, system operation was also measured in the field at the Hämeenlinna site in southern Finland for validation of the model. The model was further extended for evaluation of thermal regimes generated in the pile shaft, the results from which were used in a subsequent evaluation of the mechanical behaviour of pile foundations. One of the main objectives of Paper III was to calculate the energy efficiency of the system with and without groundwater flow effects. For this objective, a short period of imbalance in operation of the system was analysed and the results were examined in detail.

***Research task 2:** To determine the thermo-mechanical behaviour of energy piles, in terms of structural and geotechnical aspects of design and pile mechanical behaviour, in both heating and cooling operations, with a strong focus on the Finnish climate.*

These issues were evaluated in Papers I-III. In Paper I, the thermal profiles of surrounding soil and pile shaft were calculated and the data were utilised in the following steps of the research. In Paper II, the mechanical behaviour of energy piles and their bearing capacity were calculated in terms of both structural and geotechnical aspects. In Paper III, the model was used to analyse the thermo-mechanical behaviour of pile foundations with emphasis on the pile-soil interface, based on the elasto-plastic behaviour of soil materials.

2 Case studies

2.1 Summary of test pilot site

A group of five driven steel piles of 20 m length merged with GSHP systems were used in a pilot test in the town of Hämeenlinna in southern Finland (61°00'N; 024°28'E) by the Rautaruukki Corporation. The piles were extended to ground level without the presence of foundations or buildings, so the site ground surface was freely exposed to air temperature fluctuations. The piles were installed at 5-10 m spacing in order to prevent thermal interferences between adjacent piles. The test was based on real operating conditions. Thermal response test (TRT) measurements at the site were carried out by the Geological Survey of Finland (GTK) and soil properties were determined experimentally. The main soil type was classified as fully saturated clay. Measurements of heating operations started on 21 December 2011 and measurements of cooling operations on 11 May 2012. Two different types of U-tubes (single and double) were tested. The ends of the pipes at the head of the piles were connected to a small service building in the middle of the test site by well-insulated collector pipes laid on the ground surface. All systems had their own separate circulation, which enabled different variations of pile configurations and different fluid flows to be investigated (Fig. 3).

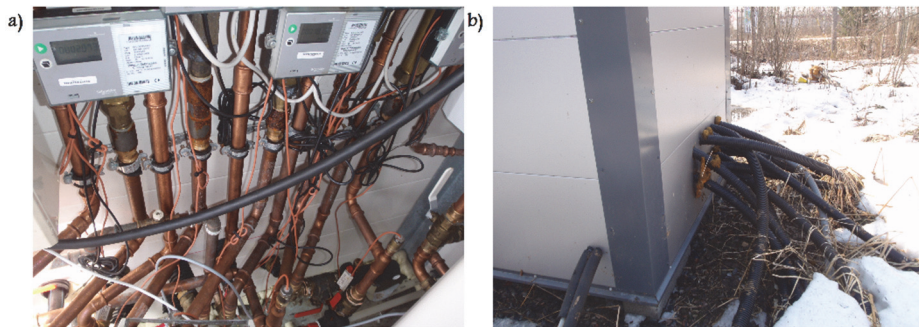


Fig. 3. (a) Measurement equipment at service building and b) collector pipes (Paper I, reprinted with permission from Journal Energy and Buildings).

3 Methodology

To examine issues concerning heat transfer in energy pile foundations and their thermo-mechanical behaviour, several simulation models were used. The software employed for the analysis of heat transfer between energy piles and surrounding environment is able to simulate heat transfer processes in GSHP systems using computational fluid dynamics with forced convection of heat carrier fluid inside the pipes, conduction in pipe walls to pile materials and conduction and convection in porous media. The finite element method used for software analysis has been employed extensively in analysis of such systems, e.g. Zanchini *et al.* [33] utilised it to calculate groundwater flow effects on performance of a borehole heat exchanger under different unbalanced conditions. Non-isothermal laminar flow conjugated with heat transfer was included in the analysis, based on main formulations of continuity, momentum and energy equations [34].

3.1 Thermal analysis

3.1.1 Model specifications

Heat transfer between GHEs and the ambient environment strongly depends on soil parameters, ground temperature gradient and the degree of soil saturation [35, 36]. In this part of the thesis work a typical type of Finnish clay soil was selected and the soil properties were based on experimental values measured in the test station at the Hämeenlinna site. Hence, the K_{eq} value used in the model was based on the measured value, in order to increase the precision of analysis. In view of the specific properties of the clay (high porosity and low hydraulic conductivity) and other on-site observations, the effect of groundwater flow on thermal regimes was neglected. Physical soil properties used in the model are shown in Table 1.

Table 1. Physical properties of materials used in the model (Modified from Paper I, with permission from Journal Energy and Buildings).

Material Parameter	Value	Unit
Soil		
Dry density (clay)	1250	kg/m ³
Fully saturated density (clay)	1812	kg/m ³
Water content	45	%
Dry heat capacity	800	J/kg K
Fully saturated heat capacity	1845	J/kg K
Fully saturated thermal conductivity	1.1	W/m K
Concrete		
Density	2400	kg/m ³
Heat capacity	880	J/kg K
Thermal conductivity	1.8	W/m K
Steel		
Steel density	7850	kg/m ³
Steel heat capacity	475	J/kg K
Steel thermal conductivity	44.5	W/ m K
HDPE (high density polyethylene)		
Density	950	kg/m ³
Heat capacity	2250	J/kg K
Thermal conductivity	0.42	W/m K

Based on the minimum distance between adjacent energy piles in the pilot test (5 m) and the average length of the steel piles (20 m), the lateral domain extension of finite volume mesh used in numerical analysis was selected as 10 m × 10 m and the height of soil domain as 30 m (L + 10 m) [37] (where L is pile length). Approximately 230,000 tetrahedral elements were employed for modelling single U-tube piles (piles 1-4 in Table 2) and around 260,000 for the double U-tube pile (pile 5 in Table 2). Meshing of domains was gradually refined in order to achieve invariable outputs of the model. Fig. 4 shows the meshing and double U-tube configuration used in numerical modelling. As can be seen, soil meshing around the pile shaft and pile meshing around the U-tubes were refined in order to increase the precision of results related to heat transfer through these zones. Physical properties of materials used in the model are shown in Table 1. The properties of fluid inside the tubes were assumed to correspond to those of water. Data on material properties of water, concrete and steel were extracted from the software material library [38]. Based on Brandl [30], the minimum fluid temperature in the

inlet of tubes during heating operations (wintertime) was kept above 0°C to prevent soil freezing effects on the system.

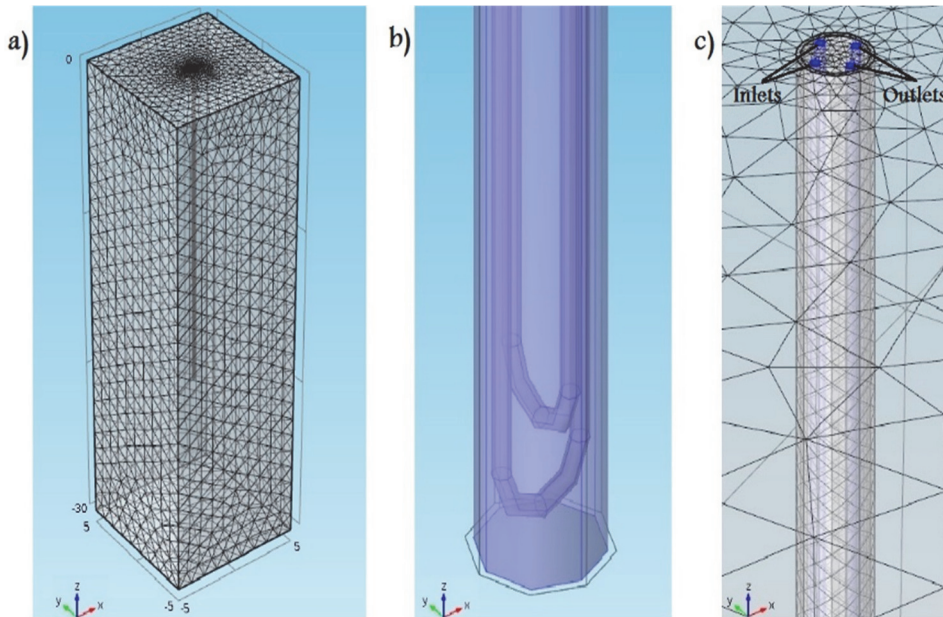


Fig. 4. a) Soil domain extension, b) double-tube configuration at the end of pile and c) meshing used around inlets and outlets of double-tubes (Paper I, reprinted with permission from Journal Energy and Buildings).

According to Brandl [30], fluid flow regimes inside the pipes of energy piles are divided into two zones, transient and steady state. The transient zone has velocity and temperature changes over the pipe length, while the steady state zone has a stable hydro-dynamic and thermal profile. Adam and Markiewics [39] found that in absorber pipes of GHEs, the steady state zone is dominant and is reached within a short distance from the tube inlet. In view of this short distance and in order to simplify the model, non-isothermal laminar flow conjugated with heat transfer was assumed in this thesis. A time-dependent analysis lasting 28 days was used to calculate the heating and cooling operations. Four types of single-tube pile (piles 1-4) and one type of double-tube pile (pile 5) were used in the heating/cooling modes. The inlet temperature of tubes started from 6°C and ended at 0°C over the 28 days for the heating mode regarding the initial ground temperature (Fig. 5) and Brandl's recommendation. This temperature changed from 8°C to 18°C and from

8°C to 55°C over two 28-day periods for the cooling modes. Ultimate temperatures 18°C and 55°C were selected based on the maximum daily average air temperature in summer time and to amplify the ground source for future use in winter time (common in cold regions), respectively. This fairly high temperature of 55°C can be achieved in practice by integrating solar heat collector pipes in the system, and was used only for analysis of thermal regimes in the pile shaft in this thesis. Thermal regimes were taken into account only for pile 1, along vertical and horizontal axes over the pile length. Geometry and physical input values for the five energy piles used in the numerical model are shown in Table 2.

Table 2. Geometry and physical input values of energy piles used in model. The first number in the pile type column relates to the outer dimensions of the pile shaft and the second the steel shell thickness, while RR indicates driven piles (Paper I, reprinted with permission from Journal Energy and Buildings).

Pile number	Pile type	Pile length (m)	Water flow rate (m ³ /h)	Inlet velocity (m/s)	Collector type
1	RR 170/10	20	0.324	0.183	Single U-tube PE 25x2.3
2	RR 170/10	20	0.324 x 1.5	0.275	Single U-tube PE 25x2.3
3	RR 170/10	20	0.324 x 0.5	0.092	Single U-tube PE 25x2.3
4	RR 170/10	20	0.324 x 2.56	0.183	Single U-tube PE 40x2.3
5	RR 170/10	20	0.324 x 2	0.183	Double U-tube PE 25x2.3

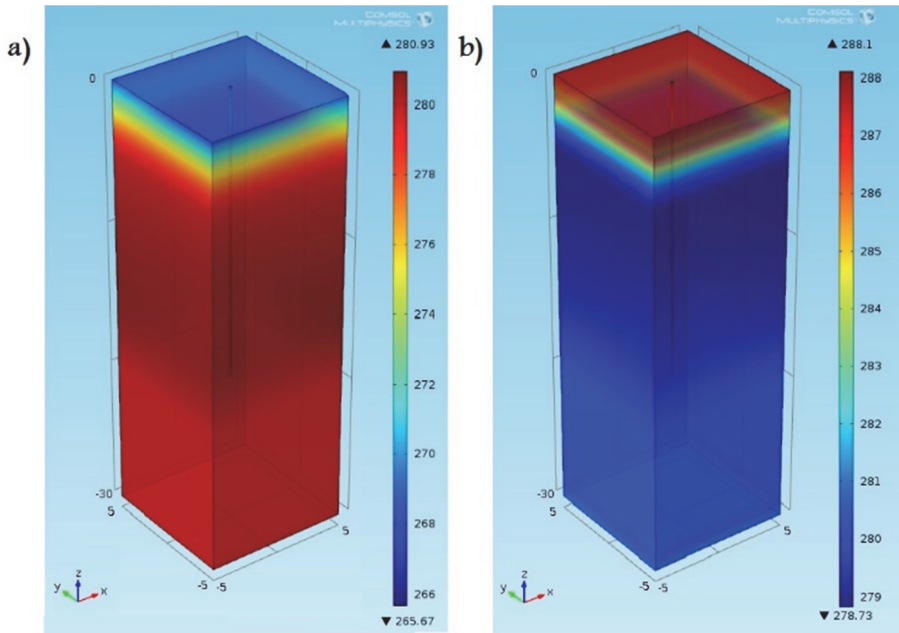


Fig. 5. Initial ground temperature used in the numerical model in a) winter mode and b) summer mode (units K) (Paper I, reprinted with permission from Journal Energy and Buildings).

Initial values and boundary conditions

Shallow geothermal potential is mainly affected by the thermal gradient between the ambient air and the ground, which induces heat transfer in the domain [40]. Seasonal temperature variations in the ground are mainly associated with depth and decrease with increasing depth below the ground surface [41]. Ground temperature values measured at different depths (down to 20 m) in the pilot test before heating and cooling operation of the systems were selected as initial values for the model (Fig. 5). It can be seen that initial ground temperature before summer mode was close to that in winter mode, which reflects the reduction in ground temperature from heat extraction during the cold season. Regarding the symmetry of the problem, the vertical boundary surfaces of the soil domain were considered adiabatic. The temperature of the lower surface of the soil domain was considered to be equal to the temperature at 20 m depth and to remain constant during the analysis, while for the upper surface mean monthly air temperature was used.

3.2 Mechanical behaviour

3.2.1 Theoretical background and governing equations

The Comsol Multiphysics package was used for analysis of heat transfer processes between energy pile and surrounding soil and for calculating the structural and geotechnical behaviour of the pile under heating/cooling thermal loadings. The Comsol package has been used previously to analyse heat transfer in energy piles and is reported to provide good reliability [42]. The ‘Free and Porous Media Flow’ interface and ‘Heat Transfer in Porous Media’ interface in the package were used for analysing the fluid flow regime inside U-tubes and heat transfer between the pile, soil and heat carrier fluid domains. The ‘Solid Mechanics interface’ coupled with the ‘Heat Transfer in Porous Media’ interface were used for analysing the structural and geotechnical behaviour of piles under heating/cooling thermal loadings [34, 43]. In the Lausanne test [13], it was observed that a linear elastic range prevailed for geotechnical behaviour of the soil at the pile-soil interface and that temperature-induced stresses in the soil domain did not extend into the range where soil friction would prevent the pile shaft from returning to its original position. Consequently, in the structural analysis, linear elastic behaviour of isotropic materials was assumed for both the pile and soil domains.

Conceptual background to the model

In theory, when a free column pile is heated it expands and when it is cooled it contracts. The magnitude of these deformations depends on the thermal characteristics of the pile shaft and can be calculated as [44]:

$$\varepsilon_{T-Free} = \alpha \cdot \Delta T \quad (1)$$

where ε_{T-Free} is pile axial thermal strain when the boundary conditions are free and the friction at the pile-soil interface is omitted.

However, the strains in free piles and constrained piles differ and for the pile-soil interface conditions and when there are restraints at pile head and toe (end-bearing pile strata or fixed super-structure), the piles are not able to expand/contact freely and thus the pile axial thermal strain when the boundary conditions are obstructed (ε_{T-ObS}) is less than the value calculated using Eq. (1):

$$\varepsilon_{T-Obs} \leq \varepsilon_{T-Free} \quad (2)$$

$$\varepsilon_{T-Rstr} = \varepsilon_{T-Free} - \varepsilon_{T-Obs} \quad (3)$$

The resisted thermal strains (ε_{T-Rstr}) induce thermal stresses in the pile shaft, such that pile axial thermal load (P_T) is calculated as:

$$P_T = -EA\varepsilon_{T-Rstr} \quad (4)$$

where a negative sign denotes compressive stresses and a positive sign denotes tensile stresses.

Background to thermo-elasticity theory

For linear elastic materials, total strain tensor (ε) can be written according to the displacement gradient as:

$$\varepsilon = \frac{1}{2}(\nabla u + \nabla u^T) \quad (5)$$

where ∇u is displacement gradient and is computed according to material coordinates as:

$$\nabla u = \begin{bmatrix} \frac{\partial u}{\partial X} & \frac{\partial u}{\partial Y} & \frac{\partial u}{\partial Z} \\ \frac{\partial v}{\partial X} & \frac{\partial v}{\partial Y} & \frac{\partial v}{\partial Z} \\ \frac{\partial w}{\partial X} & \frac{\partial w}{\partial Y} & \frac{\partial w}{\partial Z} \end{bmatrix} \quad (6)$$

According to the generalised Hooke-Duhamel law for thermo-elastic, isotropic materials:

$$s = s_0 + C: (\varepsilon - \varepsilon_0 - \alpha \theta) \quad (7)$$

where s_0 and ε_0 denote initial stress and strain, $\theta = T - T_{ref}$, α is a thermal expansion coefficient, C is the fourth order elasticity tensor and “.” denotes the double-dot tensor product.

Elasticity energy using tensor components is written according to:

$$W_s = \sum_{i,j,m,n} \frac{1}{2} C^{ijmn} (\varepsilon_{ij} - \varepsilon_{ij}^0 - \alpha_{ij}\theta) (\varepsilon_{mn} - \varepsilon_{mn}^0 - \alpha_{mn}\theta) \quad (8)$$

Due to the symmetry the stress, strain and thermal expansion tensors are written as the following matrices:

$$\begin{bmatrix} S_x & S_{xy} & S_{xz} \\ S_{xy} & S_y & S_{yz} \\ S_{xz} & S_{yz} & S_z \end{bmatrix}, \begin{bmatrix} \varepsilon_x & \varepsilon_{xy} & \varepsilon_{xz} \\ \varepsilon_{xy} & \varepsilon_y & \varepsilon_{yz} \\ \varepsilon_{xz} & \varepsilon_{yz} & \varepsilon_z \end{bmatrix}, \begin{bmatrix} \alpha_x & \alpha_{xy} & \alpha_{xz} \\ \alpha_{xy} & \alpha_y & \alpha_{yz} \\ \alpha_{xz} & \alpha_{yz} & \alpha_z \end{bmatrix} \quad (9)$$

For isotropic materials the elasticity and thermal expansion matrices are as follows:

$$D = \frac{E}{(1+\gamma)(1-2\gamma)} \begin{bmatrix} 1-\gamma & \gamma & \gamma & 0 & 0 & 0 \\ \gamma & 1-\gamma & \gamma & 0 & 0 & 0 \\ \gamma & \gamma & 1-\gamma & 0 & 0 & 0 \\ 0 & 0 & 0 & \frac{1-2\gamma}{2} & 0 & 0 \\ 0 & 0 & 0 & 0 & \frac{1-2\gamma}{2} & 0 \\ 0 & 0 & 0 & 0 & 0 & \frac{1-2\gamma}{2} \end{bmatrix}, \begin{bmatrix} \alpha & 0 & 0 \\ 0 & \alpha & 0 \\ 0 & 0 & \alpha \end{bmatrix} \quad (10)$$

Hooke's law for computation of thermal stresses according to the elasticity matrix is as follows:

$$\begin{bmatrix} S_x \\ S_y \\ S_z \\ S_{xy} \\ S_{yz} \\ S_{xz} \end{bmatrix} = \begin{bmatrix} S_x \\ S_y \\ S_z \\ S_{xy} \\ S_{yz} \\ S_{xz} \end{bmatrix}_0 + D \left\{ \begin{bmatrix} \varepsilon_x \\ \varepsilon_y \\ \varepsilon_z \\ 2\varepsilon_{xy} \\ 2\varepsilon_{yz} \\ 2\varepsilon_{xz} \end{bmatrix} - \begin{bmatrix} \varepsilon_x \\ \varepsilon_y \\ \varepsilon_z \\ 2\varepsilon_{xy} \\ 2\varepsilon_{yz} \\ 2\varepsilon_{xz} \end{bmatrix}_0 - \theta \begin{bmatrix} \alpha_x \\ \alpha_y \\ \alpha_z \\ 2\alpha_{xy} \\ 2\alpha_{yz} \\ 2\alpha_{xz} \end{bmatrix} \right\} \quad (11)$$

The thermo-elasticity equations are derived from the first law of thermodynamics [45-49]. In order to further clarify the theory, the process involved can

be explained thus: when stretching an elastic bar and increasing the stresses, the bar temperature drops reversibly and adiabatically to compensate for the entropy increase caused by stresses generated in the solid and to keep it unchanged.

The free energy equation for linear thermo-elastic material is:

$$F = \rho f_0(T) + W_s(\varepsilon, T) \quad (12)$$

where $W_s(\varepsilon, T)$ is extracted using equation (8). Therefore, the stress is calculated by the following equation:

$$s = \left(\frac{\partial F}{\partial \varepsilon}\right)_T = \left(\frac{\partial W}{\partial \varepsilon}\right)_T = C: (\varepsilon - \varepsilon_0 - \alpha \theta) \quad (13)$$

and the entropy per unit volume is calculated as:

$$-\left(\frac{\partial F}{\partial T}\right)_\varepsilon = \rho C_p \log\left(\frac{T}{T_0}\right) + S_{Elastic} \quad (14)$$

where T_0 is a reference temperature and ρC_p is volumetric heat capacity. $S_{Elastic}$ in isotropic materials is written as:

$$S_{Elastic} = \alpha : s = \alpha (s_x + s_y + s_z) \quad (15)$$

The heat balance equation is then:

$$(\rho C_p) \frac{\partial T}{\partial t} + T \frac{\partial}{\partial t} S_{Elastic} = \nabla \cdot (k \nabla T) + Q_h \quad (16)$$

where K is thermal conductivity matrix and Q_h is heat source per unit volume and is written as:

$$Q_h = S_{InElastic} : \dot{\varepsilon} \quad (17)$$

where $\dot{\varepsilon}$ denotes the strain rate tensor and $S_{InElastic}$ represents possible inelastic stresses such as viscous stress.

3.2.2 Numerical modelling

In general, two main types of energy pile sections and installations are considered in the literature, i.e. with the U-tubes installed at the centre of piles or near to the

pile shaft [50]. Consequently, when designing energy piles, the position of the U-tubes and the associated thermal regime generated in the pile shaft should be taken into consideration, as the two different thermal regimes created are able to induce two different types of pile mechanical behaviour [51].

Summary of numerical study

A steel tubular pile with concrete infill (length 20 m, diameter 220 mm) was used as the study object. A realistic GSHP system in heating/cooling operations was added to the model. The geometry and physical properties of the pile and GSHPs are shown in Table 3. The distance between adjacent energy piles was 10 m to prevent thermal overlap effects between the piles. Therefore, the lateral domain extension and soil domain height taken into analysis were defined as 10 m x 10 m x 30 m ($L + 10m$) [37], where L is pile length (Fig. 6). Model meshing consisted of 270,000, tetrahedral elements and around 994,000 degrees of freedom. Size of elements ranged from 0.3 m to 1.15 m and from 0.04 m to 0.15 m for soil and pile domains, respectively. As shown in Fig. 6, the meshing was refined in zones in the vicinity of domain junctions in order to achieve converged values in the results. The soil type was assumed to be clay and the heat carrier fluid in tubes was assumed to be water. Fluid flow regimes inside U-tubes include two zones: a transient zone with changes in velocity and thermal profile over the pile length and a steady-state zone with a constant hydrodynamic and thermal profile [42]. Considering that in U-tubes the steady-state zone is dominant and is reached within a short distance of tube inlets, in this analysis laminar flow was assumed. The thermal properties of materials used in the model were taken from the material library of the software [36] and the material properties of the soil and high density polyethylene (HDPE) U-tubes embedded in the pile shaft were chosen with reference to Hassani Nezhad Gashti *et al.* [42], as shown in Table 4.

Table 3. Geometry and physical properties of pile and ground source heat pumps. The first digit of the pile code denotes the outer diameter of the tubular steel shaft and the second digit the steel shaft thickness (Paper II reprinted with permission from Journal Engineering Structures).

Pile length (m)	Pile diameter (mm)	Water flow rate (m ³ /h)	Inlet velocity of heat carrier fluid (m/s)	Collector type
20	220/10	0.324	0.183	Single U-tube PE 25 x 2,3

Table 4. Thermal properties of the homogeneous isotropic material used in the model (Paper II reprinted with permission from Journal Engineering Structures).

Material	Density (Kg/m ³)	Heat capacity (J/kg K)	Thermal conductivity (W/m K)
Concrete	2400	880	1.8
Steel	7850	475	44.5
HDPE	950	2250	0.42
Clay	1812	1845	1.1

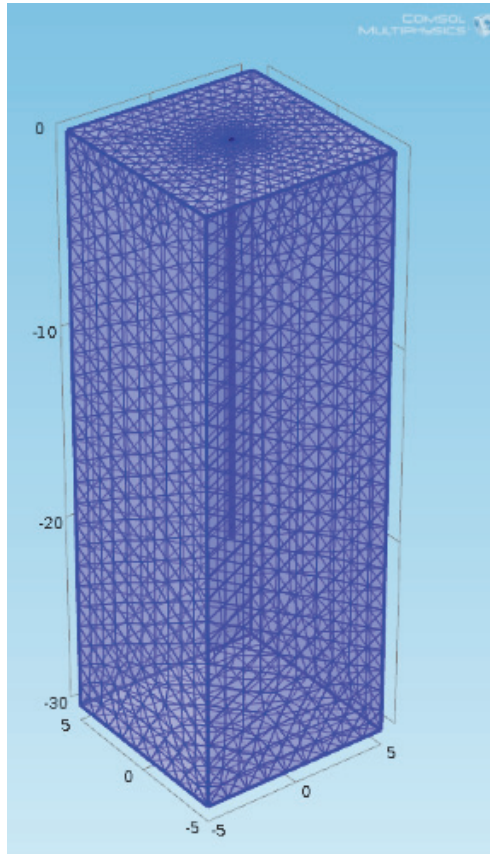


Fig. 6. Model domain extension and meshing used in the analysis (Paper II, reprinted with permission from Journal Engineering Structures).

Initial ground temperatures used in the analysis of heating/cooling operations are shown in Fig. 7. The temperature profile was selected based on thermal response test (TRT) measurements carried out at Hämeenlinna city (southern Finland, 61°00'N; 024°28'E) [42]. The initial ground temperature used at the beginning of the simulation in winter mode was also selected as the strain reference temperature used in calculation of extra thermal stresses and deformations for both contraction and expansion operations. In general, temperature variations resulting from energy pile operation do not have any detrimental effects on geotechnical soil properties [52]. Therefore, changes in soil properties with significant effects on geotechnical failure in energy piles were not taken into consideration. However, for normally consolidated soils sensitive to heating and surrounding frictional piles in particular,

this factor must be taken into consideration [53]. Owing to the symmetry of the study object and the prevention of thermal overlap effects from adjacent piles, vertical ground surfaces were considered to be adiabatic, while constant temperature was selected for the bottom surface of the soil domain and monthly air temperature for the upper surface.

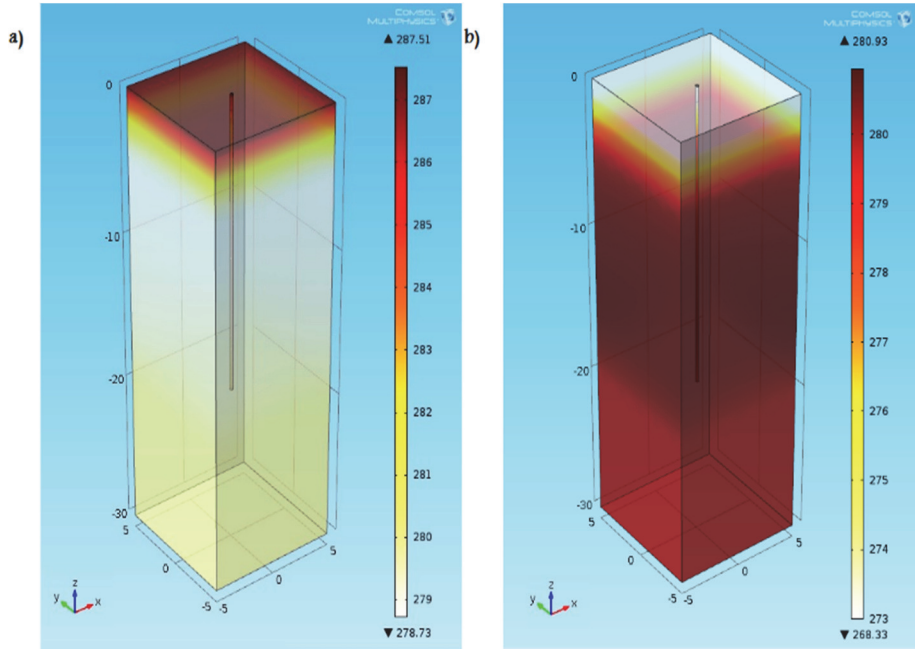


Fig. 7. Initial ground temperatures (K) used in the analysis of heating/cooling operations: a) summer mode; b) winter mode (strain reference temperature) (Paper II, reprinted with permission from Journal Engineering Structures).

Thermo-hydro-mechanical analysis and mechanical boundary conditions

Transient analysis was selected for calculating the thermo-hydro-mechanical behaviour of the pile. Static thermal loading of heat carrier fluid was applied at the U-tube inlet in both expansion and contraction operations. During contraction (winter time), the temperature at the U-tube inlet was varied linearly from 6°C to 0°C over a period of 30 days. This temperature range was selected based on the initial ground temperature measured at Hämeenlinna [42]. The soil thermal properties change considerably in freezing conditions for transfer coefficients [30].

In order to meet the Brandl recommendation to prevent soil freezing effects during operations, the minimum ground temperature was limited to 0°C [30]. During expansion (summer time), the temperature at the U-tube inlet was varied from 12°C to 27°C from days 1 to 15 and then from 27°C to 55°C from days 15 to 30. These ultimate temperatures of 27°C and 55°C were selected according to the common maximum air temperature in summer time and to amplify the ground as a source of energy production in winter time, respectively. This method is common in cold climates and the temperature of 55°C is achieved using solar heat collector pipes integrated with GHE systems [42]. Fig. 8 shows the temperature distribution in the pile and its surrounding environment at the end of simulations.

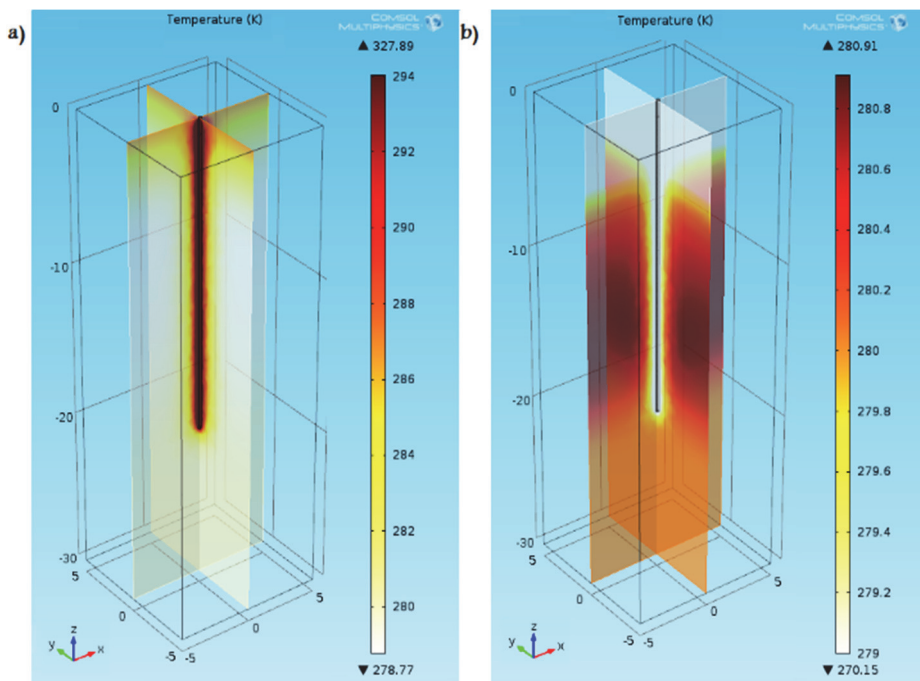


Fig. 8. Temperature (K) distribution around the pile structure at the end of simulations: a) summer mode; b) winter mode (Paper II, reprinted with permission from Journal Engineering Structures).

Pile response to vertical loads and deformations depends strongly on soil-pile interface characteristics [54, 55]. Two different contact conditions for the soil-pile interface are considered in the literature: a frictional interface, and a perfect contact interface without relative movement between pile shaft and soil. It has been

reported that thermally induced stresses are larger in the presence of perfect contact than with sliding contact [31]. It also has been observed in Lausanne tests [13] and the Lambeth College tests [56] that during heating/cooling operations piles act in a purely thermo-elastic linear way. Consequently, homogeneous isotropic linear thermo-elastic behaviour was assumed for both pile and soil domain in the present study, together with a conservative assumption of perfect pile-soil contact. The contact between concrete fill and steel shaft was also assumed to be perfect. The pile head was assumed to be fixed to the stiff superstructure, while the pile toe was assumed to bear on a stiff rock layer. Therefore, it was assumed that there was no movement at the pile head during either contraction or expansion. For the pile toe, free movement was assumed during contraction (upward movement) and no movement during expansion (downward movement) due to the presence of a stiff rock layer under the pile toe (depth around 20 m) in Finland. As the energy pile in this part of the thesis work (Paper II) was considered to be end-bearing and not frictional pile, for the conservative assumption the effect of contraction operations on pile stresses generated in expansion mode was overlooked. In contraction operations there are always stresses in the pile shaft in reverse of expansion mode, which can reduce stresses in expansion mode. Hence, for the conservative assumption the effect of the contraction mode of the pile on thermal stresses generated in expansion mode was deliberately eliminated and each one of the operations was considered to be analysed separately.

Based on symmetry, vertical surfaces of the soil domain as shown in Fig. 6 were assumed to be rolling. The bottom surface of the soil domain was assumed to be under fixed constraint and the upper surface under free constraint. Mechanical properties of materials used in the model are shown in Table 5 (concrete properties from [13] and clay properties from [57, 58]).

Table 5. Thermo-mechanical properties of homogeneous isotropic linear-elastic materials (clay, steel, concrete) used in the model (Paper II reprinted with permission from Journal Engineering Structures).

Parameter		Average value		
		Clay	Steel	Concrete
Young's modulus (MPa)	E	15	200e3	32e3
Shear modulus (MPa)	G	5.62	75e3	12e3
Coefficient of thermal expansion (1/K)	α	5e-6	1.23e-5	1e-5
Poisson ratio	ν	0.33	0.33	0.33
Coefficient of earth pressure at rest	K_0	1	-	-
Angle of internal friction (°)	ϕ	30	-	-
Cohesion (kPa)	C	15	-	-

3.3 Groundwater flow effects

3.3.1 Equations used in the model

For the simulation of heat transfer in soil and pile domains and thermo-mechanical behaviour of piles, the ‘Free and Porous Media Flow’ interface coupled with the ‘Heat Transfer in Porous Media’ and ‘Solid Mechanics’ interfaces were used. The finite element method has been widely used for such analyses and the results demonstrate good reliability [33,42,59]. Calculation of fluid flow inside the pipes was as described by Gashti *et al.* [42], while for laminar flow in porous media the Brinkman equations were used [60,61]:

$$\frac{\partial}{\partial t}(\varepsilon_p \cdot \rho) + \nabla \cdot (\rho u) = Q_{br} \quad (18)$$

$$\frac{\rho}{\varepsilon_p} \left(\frac{\partial u}{\partial t} + (u \cdot \nabla) \frac{u}{\varepsilon_p} \right) \quad (19)$$

$$= -\nabla p + \nabla \cdot \left[\frac{1}{\varepsilon_p} \{ \mu(\nabla u + (\nabla u)^T) - \frac{2}{3} \mu(\nabla \cdot u) I \} \right]$$

$$-\left(K^{-1}\mu + \frac{Q_{br}}{\varepsilon_p^2}\right)u + F$$

Calculation of the structural behaviour of an energy pile was as described by Gashti *et al.* [59]. For the calculation of friction conditions between pile and soil, the static Coulomb criterion was added to the model:

$$\tau = T_{cohe} + \mu_{stat} \cdot \sigma \quad (20)$$

3.3.2 Model description

Geometry and physical properties

For modelling in real scale, a concrete pile foundation with 60 cm diameter and a 20 m long pile shaft was simulated at the centre of a soil domain measuring 10 m × 10 m × 30 m [42], without reduction in real dimensions. For the simulation of heat transfer in soil and pile domains, the ‘Free and Porous Media Flow’ interface was coupled with ‘Heat Transfer in Porous Media’. One single-tube pile was selected for analysis and the heat carrier fluid properties corresponded to those of water. The water flow rate was set to 0.324 m³/h and a polyethylene U-tube with 25 mm diameter and 2.3 mm wall thickness was used in the analysis. Time-dependent analysis was used for temperature of the heat carrier fluid at the inlet of the tube and for groundwater flow steady-state analysis was selected. The soil was assumed to be saturated, with groundwater flow velocity equal to 1.65E-8 m/s. The heat transfer model has been validated previously in numerical studies [42]. The physical properties of materials used in the model are shown in Table 6. Soil thermal properties were selected from the laboratory test data reported by Hamdhan *et al.* [62] and data on groundwater flow properties were taken from Freeze and Cherry [63]. The numerical model used for the simulations consisted of around 253,000 domain elements and 33,000 boundary elements. Finer meshing was used around the pile shaft and U-tubes in order to obtain more explicit and precise results. The meshing was refined gradually until the results remained constant.

Table 6. Physical properties of materials used in the model (Modified from Paper III, with permission from Journal Energy and Buildings).

Material: Parameter	Value	Unit
Soil:		
Dry density (clay)	1613	kg/m ³
Bulk density	2010	kg/m ³
Water content	24.6	%
Saturated specific heat capacity	1632	J/kg K
Saturated thermal conductivity	2.75	W/m K
Porosity	40	%
Groundwater flow velocity	1.65E-8	m/s
Concrete:		
Density	2400	kg/m ³
Heat capacity	880	J/kg K
Thermal conductivity	1.8	W/ m K
HDPE (high density polyethylene):		
Density	950	kg/m ³
Heat capacity	2250	J/kg K
Thermal conductivity	0.42	W/m K

Initial values and thermal boundary conditions

The initial ground temperature profile was created using measurements made in southern Finland (61°00'N; 024°28'E) as described by Gashti *et al.* [42]. It was assumed that the ground surface was exposed to outside air temperature variations and that a constant temperature prevailed at the bottom of the 30 m deep soil domain. For vertical boundaries, adiabatic conditions were selected according to the symmetry of soil and pile (as representative of a pile group). The system was simulated using the real operating conditions in service mode in Finnish climate conditions and the actual heating/cooling operation of building spaces. Hence, a six-month heating operation starting in October was considered, following a sinusoidal algorithm with peak day at the end of December (middle day of heating period). After these first six months of heating operation, there was a two-month break in April and May when the heat exchanger was turned off. The heat pump system then worked in cooling operation for two months from the beginning of June to the end of July. After the cooling period, the system was turned off again, as there is no need for heating or cooling in Finland in August and September. The system started working in heating operation again at the beginning of October, ran for six months and was stopped at the end of March. The sinusoidal algorithm for

heat carrier fluid temperature in winter mode started from 7°C and reached a temperature of 0°C at peak day (middle of each winter mode). The latter temperature was selected according to recommendations to prevent freezing effects of soil on the system [30]. The algorithm also started from 22°C and reached 29°C at peak day in summer mode. These temperatures were selected based on the Finnish environment and the demand for air conditioning.

Mechanical properties and boundary conditions

To calculate the thermo-mechanical behaviour of piles, the ‘Solid Mechanics’ interface was coupled with the ‘Heat Transfer in Porous Media’ interface. The model has been validated previously by Gashti *et al.* [59]. For the present analysis, initial ground temperature measured in October was selected as the strain reference temperature, in order to calculate temperature-induced stresses resulting from temperature variations in pile shaft and surrounding soil. The only difference generated in this part of the analysis related to the heat carrier fluid temperature of 55°C at peak day in summer mode (day 30) and 29°C at day 15 of operation instead of day 30 in the previous part. A heat carrier fluid temperature of 55°C can be achieved in practice by using solar panels to recharge geothermal potential in summer for future usage and prevent possible system collapse resulting from long heating operation in winter. For the boundary conditions, the ground surface was assumed to be free and for the bottom surface of the soil domain fixed conditions were selected. For vertical boundaries, rolling conditions were assumed regarding the symmetry of pile and soil domain. For the pile, the head and toe were assumed to be freely supported (conservative assumption for pile head) and therefore the pile was free to expand and contract in operation. As the main focus and objective of this part of the thesis work (Paper III – Frictional pile) was on evaluation of possible collapse during thermal operation of energy piles, for the conservative assumption the pile head was assumed to be free in both operations (expansion and contraction mode). If the pile head is fixed, possible settling under operation of this heating system cannot be studied and it also makes the pile upper side incapable of movement relative to the surrounding soil. Hence, considering this conservative assumption, the pile head was considered to be free for both upward and downward movements.

For mechanical behaviour analysis of the soil domain, elasto-plastic behaviour with the Mohr-Coulomb criterion under static thermal loading was selected. For the pile-soil interface, sliding contact with possible relative movements was also

taken into account. Mechanical properties of soil and concrete used in the model are shown in Table 7. The soil properties refer to typical properties of silty-sand soil taken from the literature, while the concrete properties were taken from the Comsol material library.

Table 7. Thermo-mechanical properties of the homogeneous isotropic elasto-plastic materials and the pile-soil interface (Modified from Paper III, with permission from Journal Energy and Buildings).

Parameter		Average value		
		Soil	Interface	Concrete
Young's modulus (MPa)	E	15	-	32e3
Shear modulus (MPa)	G	5.62	-	12e3
Coefficient of thermal expansion (1/K)	α	5e-6	-	1e-5
Poisson ratio	ν	0.33	-	0.33
Coefficient of earth pressure at rest	K_0	$1 - \sin \varphi$	-	-
Angle of internal friction (°)	φ	30	10	-
Cohesion (kPa)	C	0	0	-

4 Results and discussion

4.1 Thermal analysis

The main aim of the pilot tests was to determine the performance of piles with physical properties corresponding to those of piles 1 and 5 (Table 2). In these tests, heating operations started on 21 December and the average inlet and outlet temperatures of tubes were measured until 2 January, a period of 12.75 days. A fluid flow rate of $0.324 \text{ m}^3/\text{h}$ was used during the test and the inlet temperature was kept above 0°C to prevent soil freezing effects. The simulated values of inlet and outlet temperatures of tubes for pile 1 and the corresponding values measured in the 12.75-day pilot test are shown in Fig. 9. As can be seen, there was good agreement between actual and simulated GSHP performance. This confirmed the accuracy of the simulations and indicated that the model could be used for further analyses, under various conditions, of the different types of piles listed in Table 2.

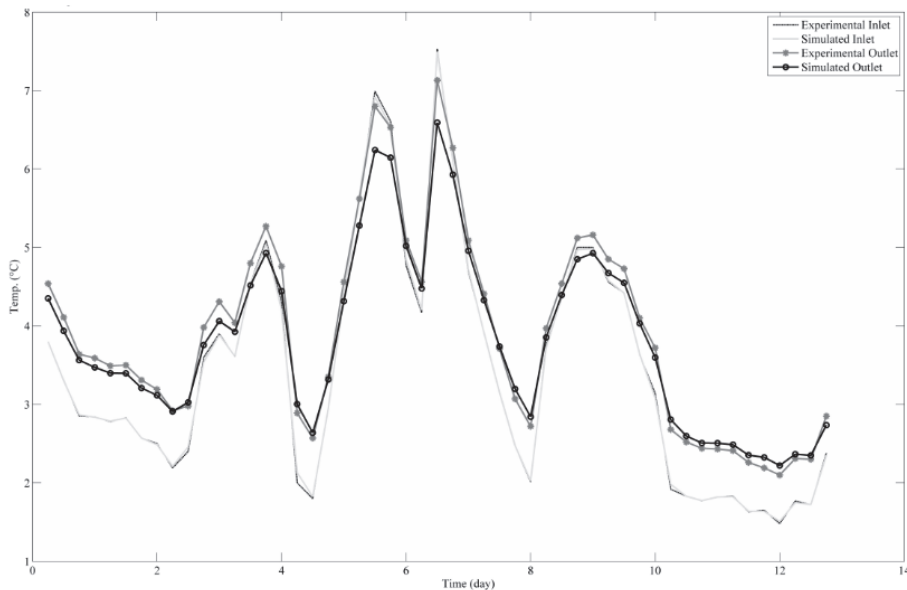


Fig. 9. Comparison of experimental and numerical values at the inlet and outlet of tubes for pile 1, 21 December 2011–02 January 2012 (Paper I, reprinted with permission from Journal Energy and Buildings).

4.1.1 Heat exchange rates of GHEs in heating and cooling operations

The model was run for all five piles listed in Table 2 for a duration of 28 days. The inlet temperature was varied from 6°C to 0°C during heating mode, while for cooling mode it was varied from 8°C to 18°C and from 8°C to 55°C during two 28-day periods. The ground temperature distribution around pile 1 at day 28 of the heating and cooling (at 55°C) modes is shown in Fig. 10, where the colour shading codes used differs between the diagrams in order to further clarify the thermal regime around the pile in the different operations. As can be seen from the diagrams, the soil domain was extensive enough to prevent thermal overlap effects between piles.

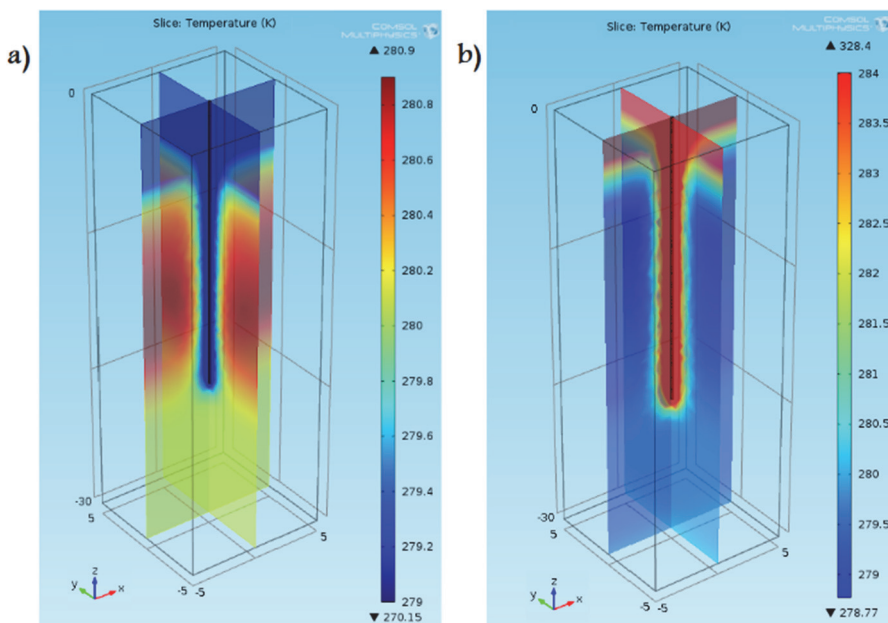


Fig. 10. Geothermal regimes around pile 1 in two orthogonal sections on day 28 of a) heating and b) cooling mode (with inlet temperature of 55°C) (Paper I, reprinted with permission from Journal Energy and Buildings).

Average inlet/outlet temperatures and differences between these during heating/cooling operations for piles 1-5 are shown in Figs. 11 and 12. At the beginning of the modelling period (first four days) in cooling operation, the system acted in reverse order and outlet fluid temperatures were partly lower than inlet

temperatures introduced to the model (Fig. 11a). This shows that over the short period of analysis for winter mode, the average ground temperature was partly lower than the inlet temperature of piles, which consequently induced a reduction in outlet temperature. It can be noted that the inlet temperature of all piles was assumed to be the same during the analyses. Therefore, the temperature differences between the inlet/outlet tubes of piles were based on equal conditions. Comparison of piles 1-3 for winter mode (Fig. 11) indicated that the highest and lowest temperature differences occurred between piles 3 and 2, where the temperature was 1.62-fold higher and 1.34-fold lower, respectively, than at pile 1 for winter mode. It proved possible to extend these results for summer mode with very close approximation, as shown in Fig. 12.

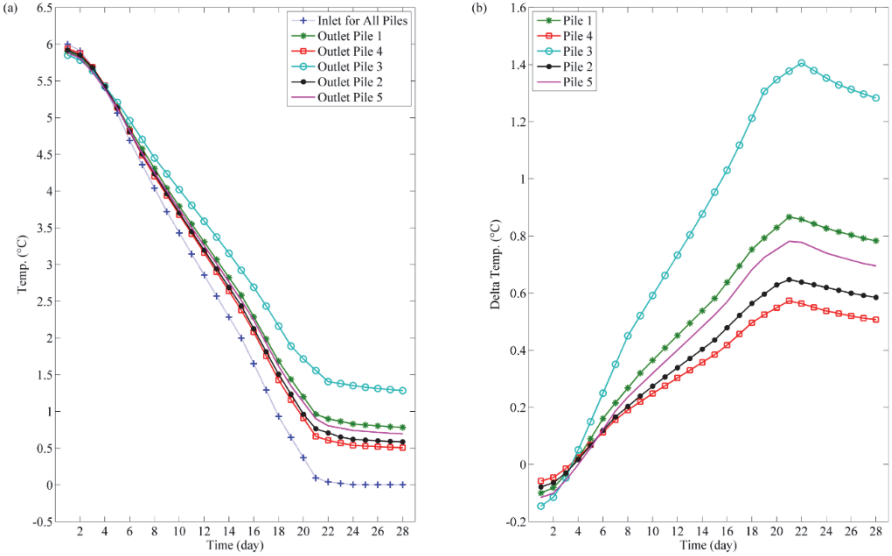


Fig. 11. Thermal performance of piles 1-5 in heating operation over the 28-day simulation period (inlet temperature variation from 6°C to 0°C): a) Inlet/outlet temperatures and b) inlet/outlet differences (Paper I, reprinted with permission from Journal Energy and Buildings).

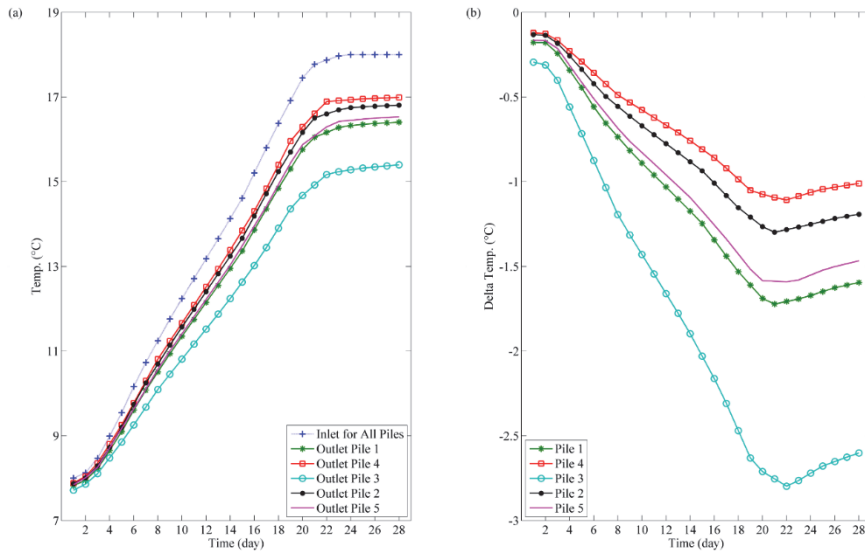


Fig. 12. Thermal performance of piles 1-5 in cooling operation over the 28-day simulation period (inlet temperature variation from 8°C to 18°C): a) Inlet/outlet temperatures and (b) inlet/outlet differences (Paper I, reprinted with permission from Journal Energy and Buildings).

The temperature differences between the inlet/outlet of tubes increased during operation of the systems until day 22 of simulations (Fig. 11b and Fig. 12b). This behaviour was the result of the greater temperature differences between tube inlets and surrounding soil created by changing the inlet temperature from 6°C to 0°C and from 8°C to 18°C for winter and summer mode, respectively. A general comparison of piles showed that at the peak points (Fig. 11b and Fig. 12b), the highest temperature difference occurred at pile 3 and the lowest at pile 4. The gradual decline in temperature differences observed after day 22 of simulation reflects the gradual reduction in geothermal potential after the constant temperature of 0°C and 18°C was reached at the inlet of tubes for winter and summer modes, respectively. This effect is more obvious for piles 4 and 5 (Fig. 13) due to the larger amount of energy extracted, and highlights the productivity dependency of GSHPs on the geothermal potential. This is in agreement with many previous studies [64-66] and demonstrates that in order to achieve viable performance of the system, the geothermal potential must first be taken into account with respect to the building energy consumption needed in future. Regarding the cold climate of Finland and

the unbalanced heat loads extracted/injected from/to the ground during winter/summer times, use of methods to reinforce the geothermal potential for sustainable performance of the system can be of great importance. One of the techniques commonly applied in cold regions can be described as solar heat collector pipes. This system, with high inlet temperature up to 55°C, is able to recover geothermal potential during summer time to prevent future collapse of the system. However, in order to achieve efficient performance of the system, extensive investigations must be carried out to prevent long operations in summer time, which can generate higher costs.

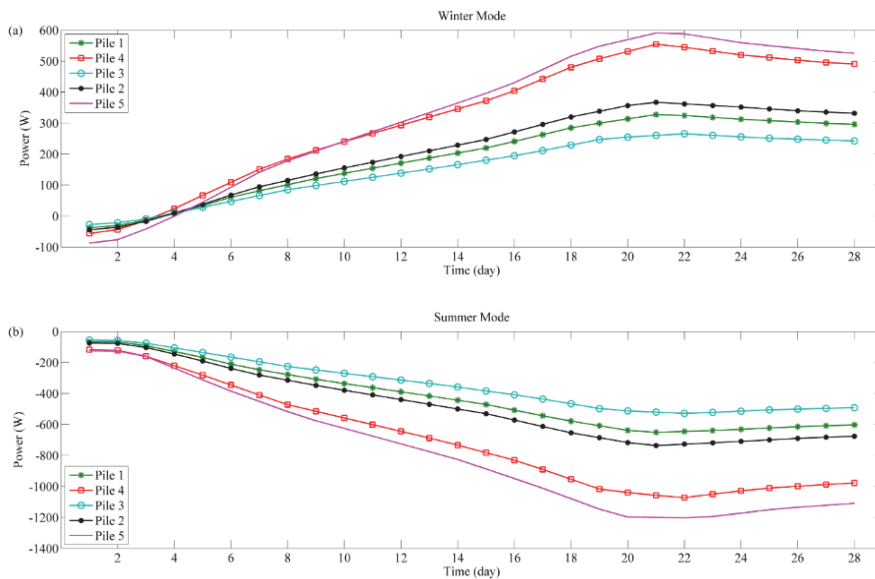


Fig. 13. Output power of piles 1-5 during the 28 days of simulation for winter and summer mode (Paper I, reprinted with permission from Journal Energy and Buildings).

Comparison of the output power values of the piles (Fig. 13) revealed that piles 5 and 3 had the highest and lowest output power, respectively. Comparing the output power of piles 4 and 5, the double-tube pile 5 was more efficient owing to its higher output power (around 10%) and lower water flow rate (28%) used in the system. This shows that to increase the output power of the system, increasing the number of U-tubes can be more efficient than increasing the tube diameter.

The output power of piles 1-3 was very similar initially, although the differences increased over the simulation period (Fig. 13). This shows that systems

with low temperature differences between tube inlets and ambient ground have little difference in their output power. Hence, to achieve tangible differences between the outputs of systems, there has to be a higher temperature difference between surrounding materials and inlet fluids. The output power ratio at peak points between piles 1 and 3 and between piles 2 and 3 for both heating/cooling operations was around 23% and 38%, respectively (Fig. 13). Consequently, as regards the ratios of fluid flow rates listed for the piles in Table 2, there was a decline in output of the systems with respect to their flow rate ratios. It is worth noting that studies concerning cost savings in the energy produced by these different systems and the cost of providing different flow rate circulations in tubes are necessary for more correct prediction of the most efficient system. Regardless of electricity costs, a primary comparison between piles 2 and 5 showed that pile 5 was more efficient with its 60% higher energy production and only 33% increase in flow rate of the system (expenses relating to water flow production are much less than those relating to the heat energy produced by systems).

4.1.2 Thermal regime in pile shaft

The thermal regime in pile shaft 1 at the end of heating operations (day 28) showed a high temperature concentration around the U-tube of the pile. The fluid temperature in the inlet was less than in the outlet and the temperature gradually increased over the tube length owing to the GSHP operating in heating mode. Vertical thermal regimes at the centre and in the vicinity of parallel pipes (points A, B and C in Fig. 1) over the pile length on the last day of heating/cooling operations (day 28) are shown in Fig. 14. Inlet temperatures of 0°C and 55°C correspond to the last day of winter and summer mode, respectively, in simulations. After a fairly long distance (three-quarters of pile length), the temperature in heating and cooling operations tended to be constant at a value of around 2°C and 43°C, respectively. On first impression, the difference between inlet fluid temperature (0°C and pile constant temperature 2°C) in winter time does not seem to be of great importance, but in view of the difference between inlet temperature and average ground temperature (around 6°C, a temperature difference of 2°C can be substantial (33% difference)). The difference between inlet fluid and pile constant temperature in cooling mode was around 12°C (25% difference). This indicates that in piles with a higher temperature difference between inlet fluid and ambient ground, pile constant temperature will be proportionately closer to inlet fluid temperature. Vertical temperature variations after around three-quarters of pile length can be

neglected except at depth under the U-curve (around 20 m depth), where there were sudden high fluctuations in temperature. These fluctuations were around 1.5°C and 11°C for winter and summer mode, respectively (Fig. 14) and were the result of high temperature concentrations occurring in the vicinity of the U-curve at the end of the pile. There was also a fairly high temperature fluctuation of around 15°C in the first 1 m of pile length in cooling operations. This fluctuation can be explained by high temperature difference between inlet fluid and ground surface around the pile in this mode, which can affect the pile temperature profile down to around 1 m depth. These fluctuations are of great importance considering the short distance of pile length over which they occur.

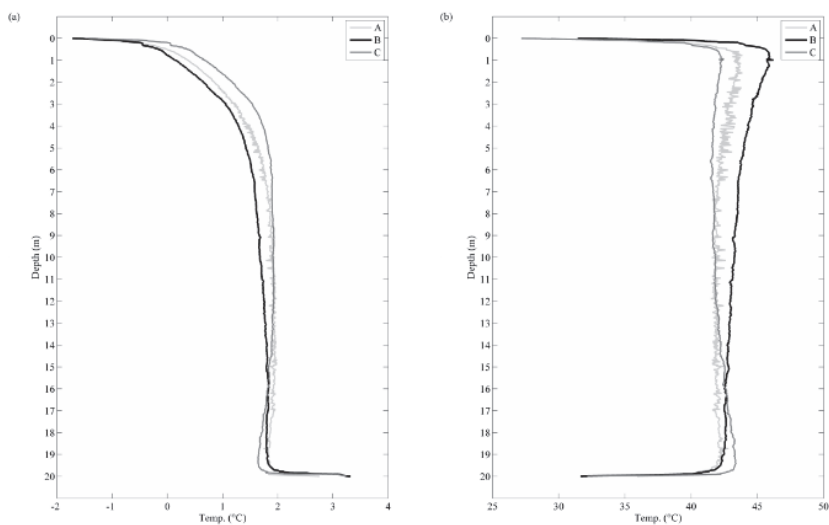


Fig. 14. Vertical temperature variations over the pile length at points A, B & C (cf. Figure 1) in a) winter and b) summer mode (Paper I, reprinted with permission from Journal Energy and Buildings).

4.2 Mechanical analysis

The model developed in this thesis was validated using empirical data obtained in experimental tests carried out in Lausanne, Switzerland [13]. The Lausanne test report is considered a significant data source in the field of thermo-mechanical behaviour of energy piles. The test was conducted on an in situ concrete pile foundation constructed on very stiff sandstone, restrained at the head by

superstructure weight. Bored piles 880 mm in diameter and 25.8 m in length were used and the soil stratigraphy was specified as five layers to a depth of 30 m. The thermo-mechanical properties of these five soil layers, as measured in the Lausanne test, are shown in Table 8.

Table 8. Thermo-mechanical properties of soil layers according to the Lausanne test (Paper II, reprinted with permission from Journal Engineering Structures).

Soil Layer	Depth (m)	Density (kg/m ³)	Bulk modulus (MPa)	Shear modulus (MPa)	Friction angle (°)	Cohesion (kPa)	Coefficient of thermal Expansion (1/K)
1	5.5	2000	122	113	30	5	1e-5
2	12	1950	122	113	27	3	1e-5
3	21.5	2000	59	1000	23	6	1e-4
4	25.8	2200	83	1400	27	20	1e-4
5	30	2550	620-3100	550-2800	-	-	1e-6

The elastic modulus of concrete based on laboratory test results was found to be 32 GPa, while for the pile by considering the elastic modulus of steel it was estimated as 29.2 GPa. Eight different tests under different thermal regimes and restrained conditions at the pile head were carried out. From these, test 7 was selected for use in validation of the numerical model in this part of the thesis work. Material characteristics, geometry, bearing conditions at head and toe, and soil stratigraphy of the experimental test were used for the analysis and the temperature change in heating operation, which was equal to +15 °C, corresponded to values used in test 7. In the procedure, the model was first constructed based on properties used in the study. Then for validation of model, the properties and geometry introduced to the programme were changed based on the Lausanne test results, to compare the results with the same conditions. Maximum vertical thermal stresses in the experimental test were observed to be equal to -2.35 (MPa) at the middle of pile length and -2 (MPa) at the pile toe. In the simulation model, these stresses were calculated to be equal to -2.3 (MPa) and -2 (MPa), respectively. From the observations, it was concluded that there was good agreement between experimental test and numerical model, as the simulation model for validation corresponded exactly to the properties and geometry of the in situ test. This agreement confirms that the model can be used for further thermo-mechanical analysis of such structures under different geometry and thermo-mechanical conditions.

4.2.1 Temperature-induced stresses

In the absence of frictional shaft resistance, piles with free supported boundary conditions at the head and toe can freely expand/constrict under temperature variations over the pile length, without generating additional thermal stresses. However, this assumes there is no temperature gradient between points located along a cross-section of pile, which could induce extra stresses owing to the unequal thermal strains. In cases where piles are not quite free to move due to constraints at the head and toe or frictional shaft resistance, some or all thermal deformations (strains) in the piles are prevented. These prevented strains induce additional thermal stresses, the value of which varies significantly depending on the degree of pile restriction at head, toe and frictional shaft and the temperature variations occurring in the pile shaft. The thermal response mechanism of piles in expansion/contraction operations regarding the two different constraint conditions at head and toe is shown in Fig. 15.

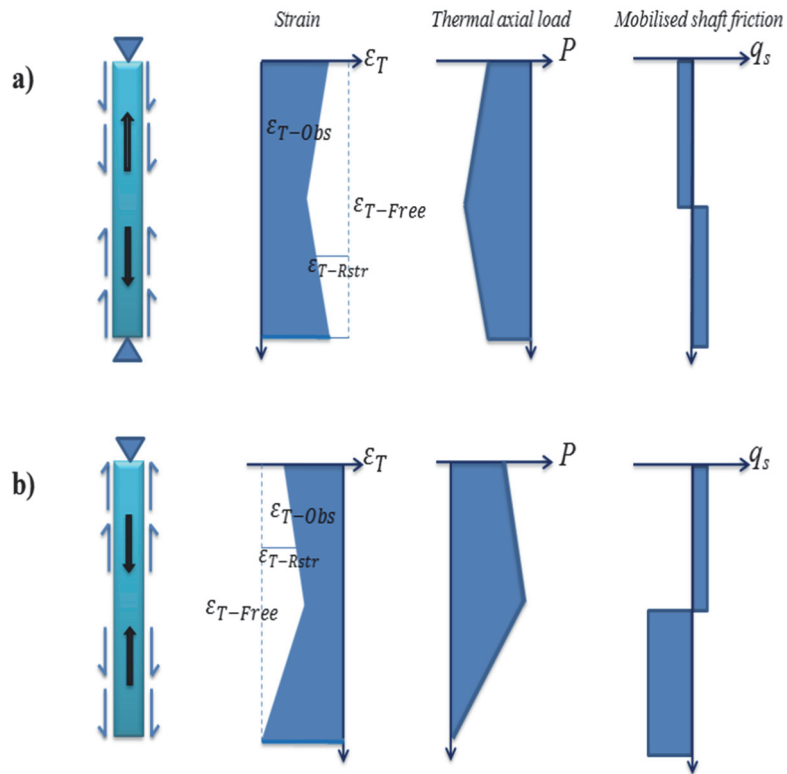


Fig. 15. Thermal loading mechanisms of the pile in different end constraint conditions under surrounding ground effects: a) fixed supported ends (expansion operation); b) fixed supported head and free supported toe (contraction operation) (Paper II, reprinted with permission from Journal Engineering Structures).

Free and fully restrained boundary conditions are typically considered for design purposes, but in reality the actual behaviour of a pile is somewhere between these extreme conditions [67]. In fully restrained behaviour, no thermal displacement can occur at the head and toe of the pile and therefore the potential movement of the pile is manifested as additional thermal stresses over the pile structure. In this thesis, the conservative assumption of fully restrained behaviour of the pile was adopted. However, Hassani Nezhad Gashti *et al.* [42] found that the temperature variations are more obvious in the vicinity of U-tubes embedded in the pile shaft. Therefore to take this into account, further axial thermal stresses were assumed to arise in the vicinity of the U-tubes embedded in the pile shaft. Axial thermal stresses generated

in different locations of the pile cross-section in heating/cooling operations are shown in Fig. 16. Three zones were distinguished in the thermal stress profile over the pile length; two transient zones with high fluctuations at top and toe of the pile and a stabilised zone at the middle. The simulation results showed that the maximum tensile/compressive stresses generated in the concrete part of the pile during both expansion and contraction occurred at locations near to downward and upward pipes (points B and C, respectively, in Fig. 16). This behaviour resulted from higher temperature variation at these locations with respect to the strain reference temperature than at other locations. This higher temperature variation was induced by fluid circulation in the U-tubes within the pile, which started at the inlet and ended at the outlet of tubes. The first transient zone at the top of pile (approximately top 1.5 m) was due to the ground surface temperature in this zone being used as the strain reference temperature. The maximum stresses generated in this zone were calculated to be around +0.6 MPa and -7 MPa for contraction and expansion operations, respectively. This first transient zone then reached a stabilised zone (dominant zone), in which the highest stresses were calculated to be +0.6 MPa and -5.7 MPa for contraction and expansion operations, respectively. These occurred at a depth of around 6 m (approximately one-third of pile length). It was observed that these stresses in the stabilised zone decreased gradually over the pile length, as a result of a gradual increase/decrease in temperature over the pile length during contraction/expansion operations. Consequently, differences between pile and strain reference temperature decreased over this zone and induced a slight reduction in stresses. The second transient zone, at the bottom of the pile, was due to the temperature concentration generated under the U-pipe curve in this zone, which can induce higher thermal stresses, as discussed by Hassani Nezhad Gashti *et al.* [42]. The maximum thermal stresses generated in the transient and stabilised zones of the pile length with inlet temperature 55 ° C were calculated to be -18 MPa and -13 MPa, respectively (Fig. 16c).

The simulation results further indicated that the lowest thermal stresses in the concrete part of the pile occurred in the vicinity of the steel shaft (points D and E in Fig. 16) in both operations. This was because of the higher thermal expansion coefficient of steel than concrete, which induced greater contraction/expansion of the steel shaft than of the concrete during contraction/expansion. These extra deformations in steel compared with concrete resulted in reverse stresses in the surrounding concrete. Consequently, tensile/compressive stresses generated in the concrete by contraction/expansion were slightly offset by the behaviour of the steel shaft. This behaviour was more obvious at the bottom of the pile in winter mode

(contraction), which induced negative stresses for points D and E from depth 16 m down to 20 m (Fig. 16). Stresses in the steel shaft were calculated to be approximately 5 MPa in contraction mode, but in view of the high ultimate yield strength of steel, when summarising the results these stresses were not taken into account in detail.

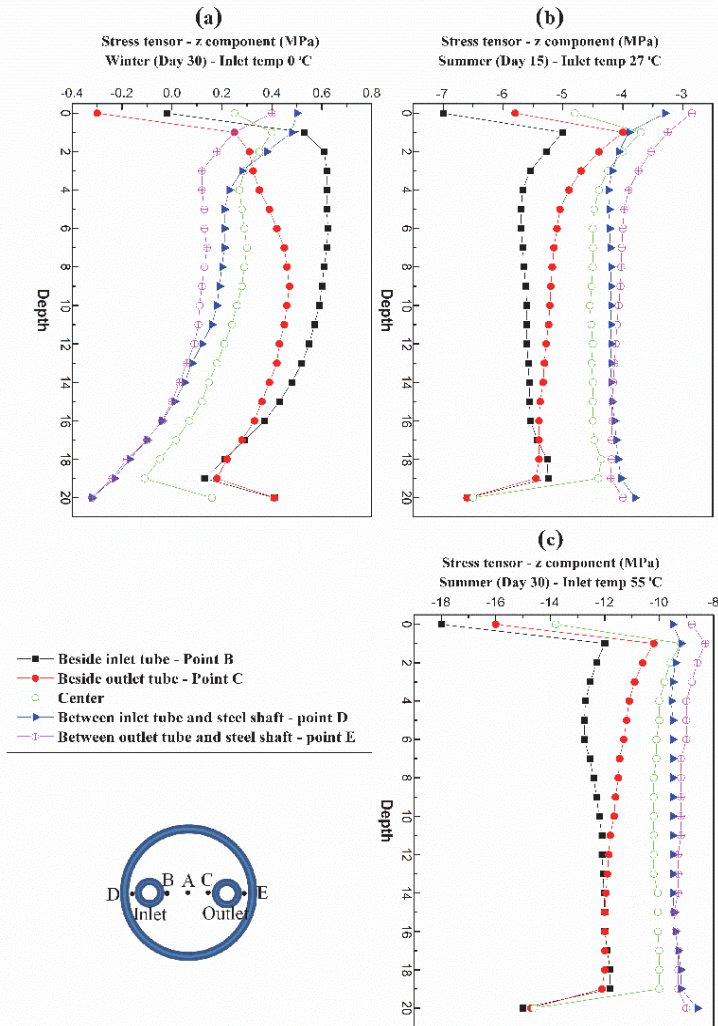


Fig. 16. Axial thermal stresses over the pile length at different points of pile cross-section: a) winter mode (inlet temperature 0°C); b) summer mode (inlet temperature 27°C); c) summer mode (inlet temperature 55°C). Tensile stresses are represented with a positive sign and compressive stresses with a negative sign (Paper II, reprinted with permission from Journal Engineering Structures).

4.2.2 Temperature-induced displacements

Theoretically, when a pile heated or cooled it expands or contracts, resulting in additional displacements in pile structure. Different pile-soil contact conditions and end-bearing strata resist part of these displacements, and as a result they arise somewhere between the cases of free and fully restrained.

Displacements over the pile length during contraction on days 1, 10, 15, 20 and 30 of simulation are shown in Fig. 17. During contraction of the pile in winter mode and with fixed constraint at the pile head due to superstructure connection, the displacements occurred in parts below the pile head and the pile mostly moved upward due to the contraction operation and free constraint at the pile toe (Fig. 17). The simulations showed that during contraction, the null point (zero-displacement point) at the beginning of the analysis was close to the bottom of the pile, but over the course of the simulation and with a decrease in inlet fluid temperature from 6° C to 0° C the null point moved upward. This behaviour was observed in piles restrained at the head and free at the toe (in contraction). It was also found that maximum displacement of the pile, around 0.7 mm, occurred at the toe at inlet fluid temperature 0° C (day 30). This result is in good agreement with findings obtained in previous numerical analyses [31].

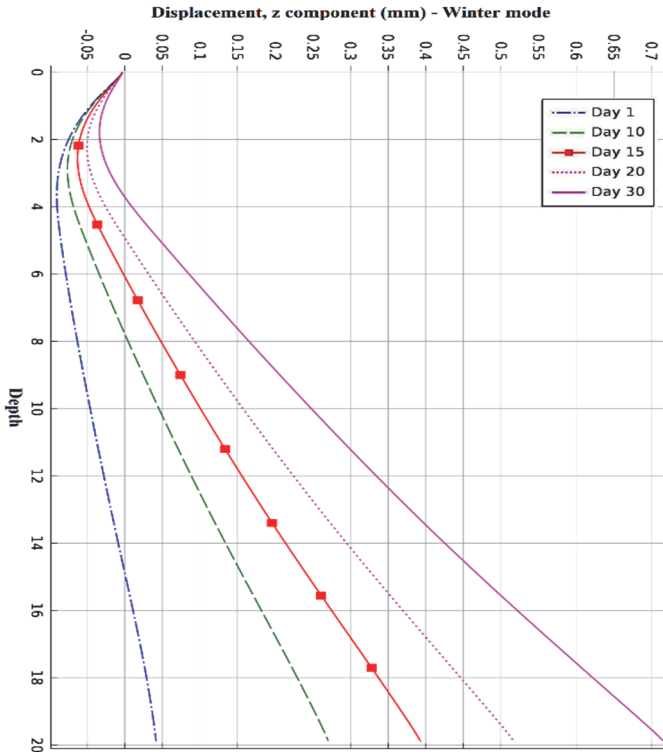


Fig. 17. Vertical displacements (z component) over the pile length in winter mode (days 1, 10, 15, 20 and 30 of simulation). Displacements with a positive sign denote upward movement and those with a negative sign downward movement (Paper II, reprinted with permission from Journal Engineering Structures).

Displacements over the pile length in summer on days 1, 10, 15, 20 and 30 of simulation are shown in Fig. 18. During expansion of the pile with fixed constraint at the head and toe (presence of stiff layer under pile toe), no tangible variation in null point location was observed over the simulation. The position of this null point was found to be very close to the pile toe. Maximum downward displacement occurred at depth 4 m and the location of this point did not change over the simulation. Maximum displacement was found to be around 0.26 mm, but decreased over the simulation with increasing pile temperature. This decrease was caused by an increase in pile displacement between around 17.6 m and 19.6 m depth. It was also observed that the displacements in points at these depths remained constant over the simulation.

The research results showed that temperature-induced deformations of the pile were negligible and could not have much effect on common building structures. However, for structures very sensitive to settling or heave, these deformations must be taken into consideration in the design context. It is also strongly recommended to avoid exposure of energy pile foundation surfaces to temperatures below freezing (less than $+2^{\circ}\text{C}$), which can cause severe heave of base slabs and in subsequent thawing periods and with loss of ground strength, settling in buildings is very possible [30].

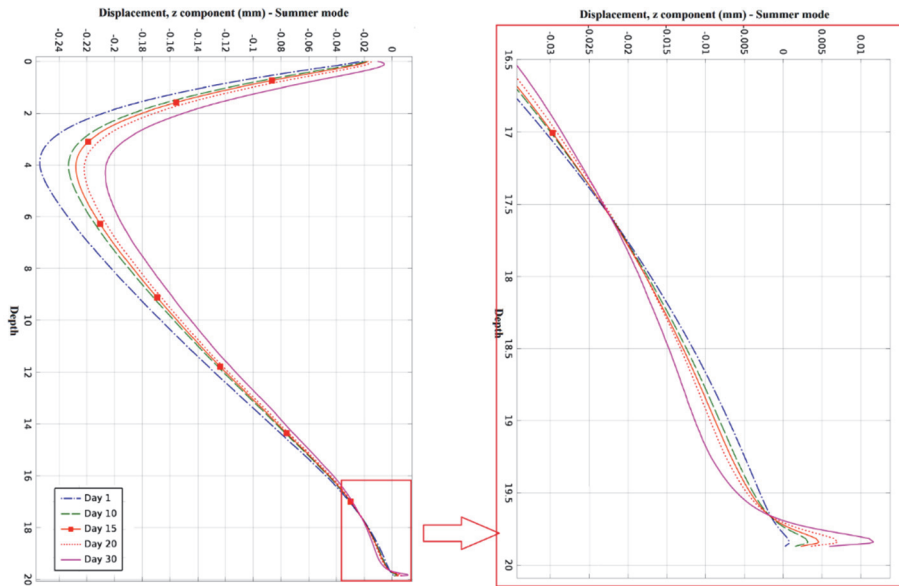


Fig. 18. Vertical displacements (z component) over the pile length in summer mode (days 1, 10, 15, 20 and 30 of simulation). Displacements with a positive sign denote upward movement and those with a negative sign downward movement (Paper II, reprinted with permission from Journal Engineering Structures).

It is worth mentioning that soil stiffness in practice is highly non-linear and the stiffness at the smallest strains and in particular after stress reversal is much higher than for the largest strain conditions. The thermal loading cycle can induce both stress reversals and the strains have remained so small (Figs. 17 & 18). The observations show that by considering the small strains in both heating/cooling operations, the soil stiffness assumption may be used for further investigations in alternate operations.

4.2.3 Mobilised shaft friction

Mobilised shaft friction at the pile-soil interface was induced by shear strains occurring under different displacements at the pile shaft and surrounding soil. In this study, perfect contact conditions at the pile-soil interface (no relative movements between pile and surrounding soil) were assumed in simulations. Ultimate shaft resistance of energy pile foundations is not affected by heat transfer between pile and surrounding soil in the statically relevant range [30]. Therefore, variations in the ultimate shaft resistance under different thermal loadings were neglected in this analysis. Temperature-induced mobilised shaft friction during heating/cooling thermal loadings is shown in Fig. 19. During cooling (contraction), increasing (positive) values were observed over the upper part of the pile and negative values over the lower part. During heating (expansion) the values were very close to zero along most of the pile length, although there were two very small fluctuations at the head and toe of the pile. These fluctuations during heating were due to high fluctuations in temperature in these zones. These results reflect the dual behaviour of the pile toe in expansion/contraction, i.e. fixed constraint in expansion and free in contraction. This mechanism of mobilised shaft friction occurs in piles lying over a stiff layer at the toe, i.e. restrained from expansion but free to contract (end-bearing piles). The maximum value of mobilised shaft friction occurred at the pile toe during winter mode and at the pile head during summer mode. The depth at which mobilised shaft friction was zero for contraction on day 30 of simulation was 8 m lower than the null point depth. The maximum displacement occurring at the pile toe was equal to 0.7 mm in winter and close to zero in summer, whereas the mobilised shaft friction at the toe was much larger in winter than in summer. This shows that the variation in mobilised shaft friction can be of much greater importance for frictional piles than end-bearing piles and can cause a significant reduction in the geotechnical resistance of frictional piles.

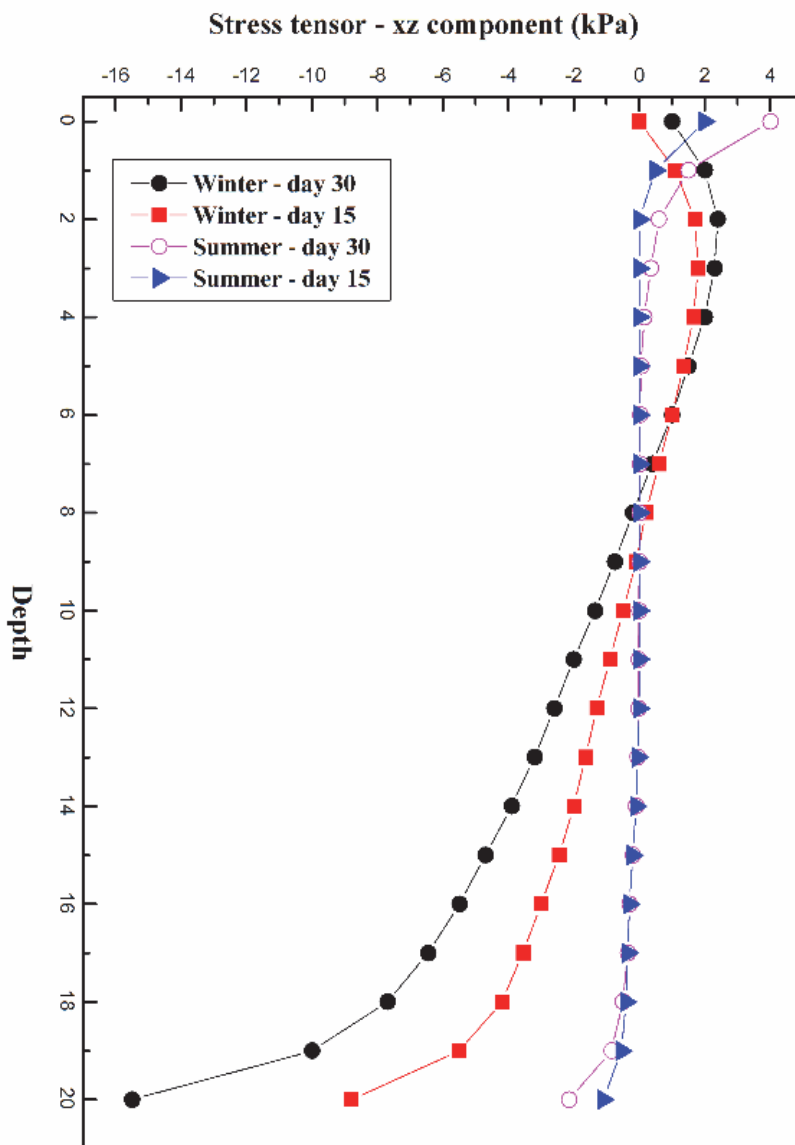


Fig. 19. Mobilised shaft friction at the soil-pile interface in summer/winter mode on days 15 and 30 of simulation. A positive sign denotes increasing friction mobilised at the pile shaft (available from pile installations), while a negative sign denotes decreasing shaft friction (Paper II, reprinted with permission from Journal Engineering Structures).

4.3 Energy piles under groundwater flow effects

4.3.1 Energy production

In energy production analysis of the system two different conditions, with groundwater flow effects and without groundwater flow, were taken into account. Figs. 20 and 21 show the ground temperature profiles around the pile at peak days of operation with and without groundwater flow effects. As can be seen, in the presence of groundwater flow the soil thermal potential around the pile in extracting/injecting heat was higher than without groundwater flow effects.

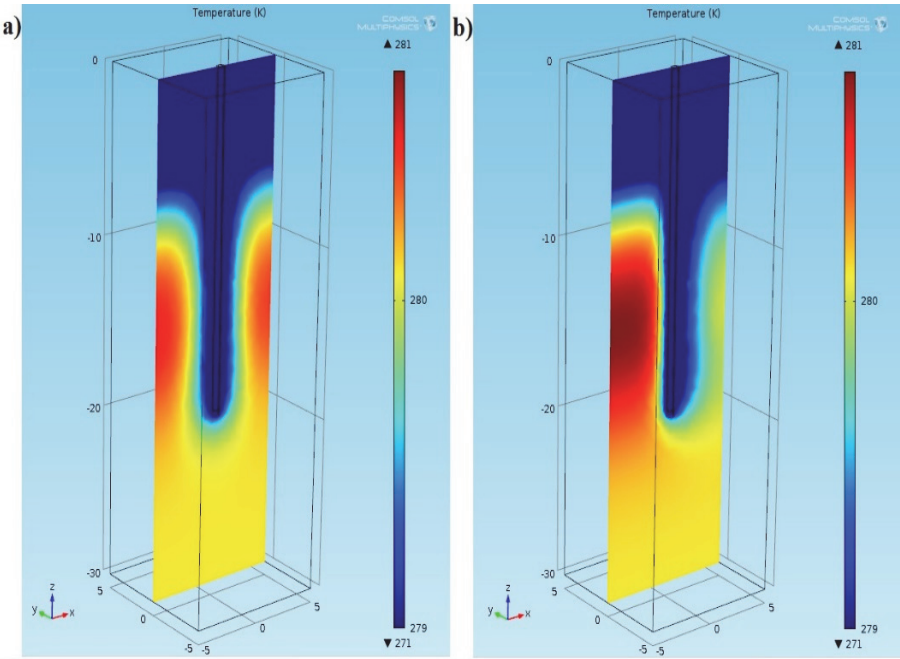


Fig. 20. Ground temperature profile around the pile shaft at peak day of heating operation (winter mode): a) without groundwater flow and b) with groundwater flow (Paper III, reprinted with permission from Journal Energy and Buildings).

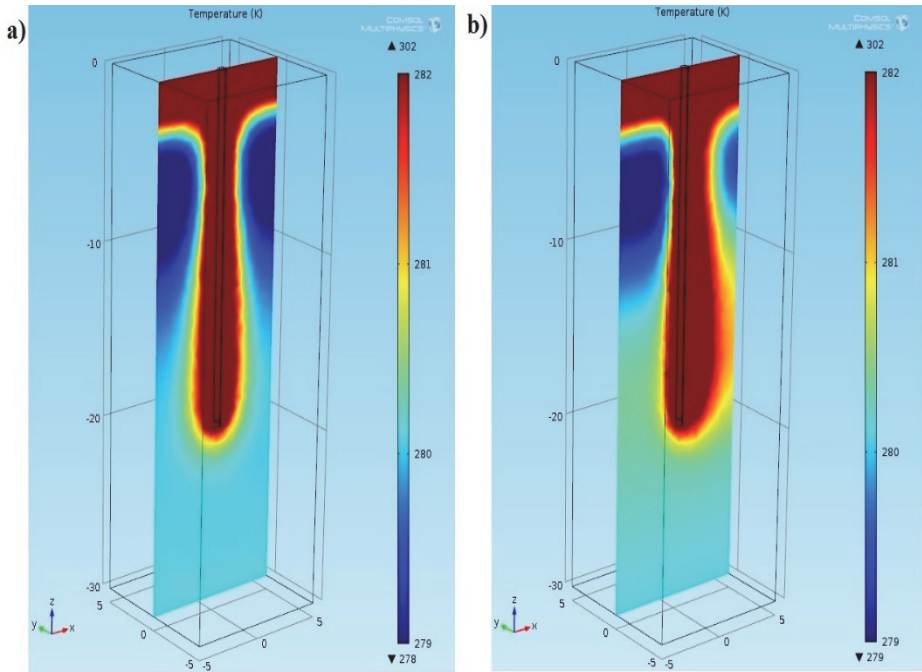


Fig. 21. Ground temperature profile around the pile shaft at peak day of cooling operation (summer mode): a) without groundwater flow and b) with groundwater flow (Paper III, reprinted with permission from Journal Energy and Buildings).

The output power of the system under heating/cooling operations (for two winter modes and one summer mode in between) is shown in Fig. 22. At the beginning of operation there was no significant difference between the two different conditions (with or without groundwater flow), which is attributable to negligible differences between the heat carrier fluid temperature in U-tubes and the ground temperature profile. With continuing system operation and larger temperature differences between heat carrier fluid and surrounding soil, the differences between systems operating with and without groundwater flow effects became more obvious. The maximum difference in energy production under the two different conditions in the first winter was observed to be around 20%. The duration of winter mode was set at 180 days, and the differences between the systems with and without groundwater flow were more obvious after the middle of each winter (from day 90 to 180). These results reflect poor potential of the ground as a heat source in winter mode, particularly in the latter half of this mode period.

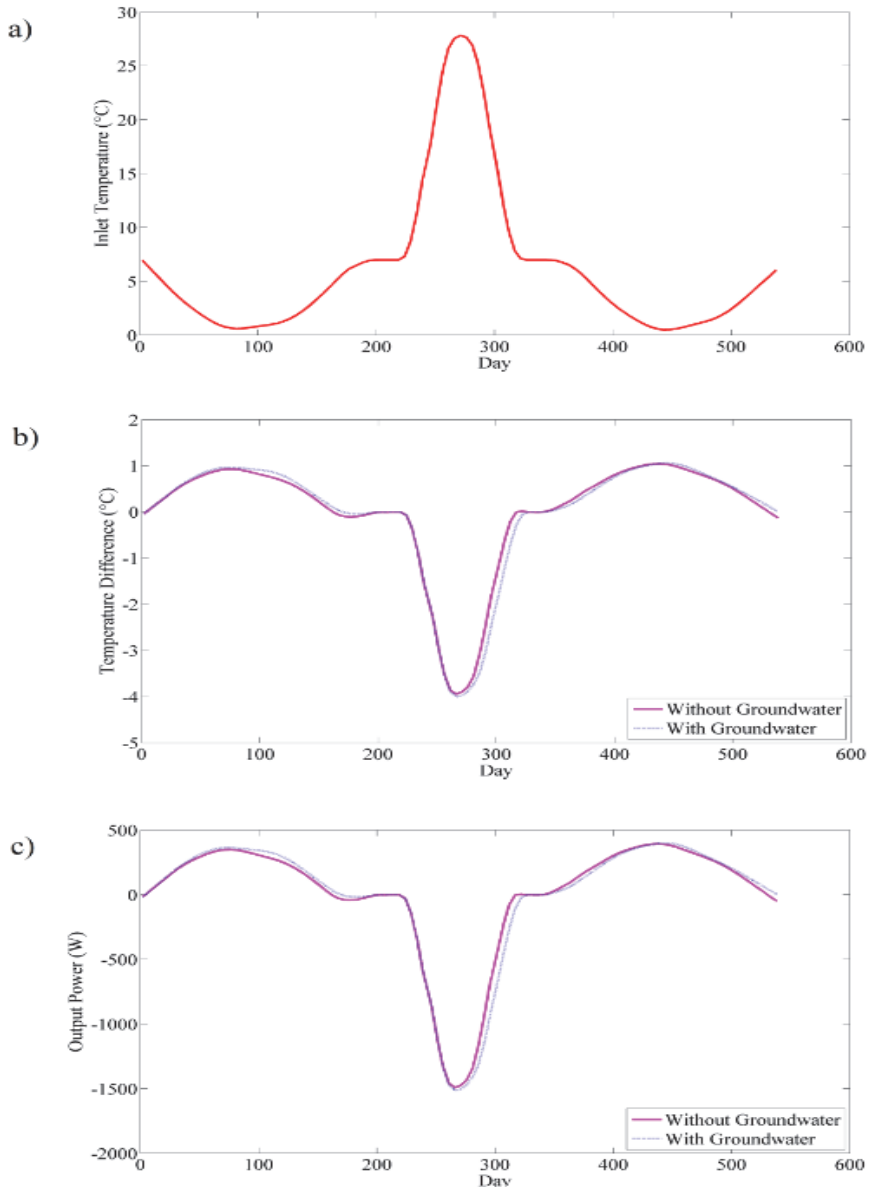


Fig. 22. System performance with and without groundwater flows. a) Inlet temperature at tubes, b) temperature difference between outlet and inlet of tubes and c) output power of systems (positive sign denotes heat extraction and negative sign heat injection) (Paper III, reprinted with permission from Journal Energy and Buildings).

The summer mode started two months after the end of the first winter mode, at day 240 of simulation. This mode operated for two months, but there was no obvious difference between the conditions with and without groundwater at the beginning of operation. This reflects high potential of the ground to be injected with heat, i.e. act as a heat sink. This difference remained negligible up to the peak day of summer mode operation, after which the differences between the two conditions were more obvious and increased with continuing system operation. The maximum difference between the systems with and without groundwater flow conditions was observed to be around 5%. This relatively small difference reflects high potential of the ground to absorb heat, i.e. act as a heat sink, and shows that groundwater flows have more significant effects on systems installed in ground with a lower potential for heat injection/extraction.

The system operation was stopped for two months after summer mode and started again for six months for the last winter mode. The system with groundwater flow had relatively lower productivity at the beginning of operation. This was the result of dissemination of energy stored in the ground in summer mode to points at a greater distance from the pile shaft, which lowered the geothermal potential of the ground around the pile at the beginning of the next winter. This proves that in ground with water flow conditions, installation of energy piles coupled with heat-solar panels during summer mode in order to store the heat in the ground for future extraction in winter is less productive. After the peak day of winter mode, the productivity of the system with groundwater flow was observed to be higher than that of the system without water flow. It was also observed that at days near the end of operation in winter mode and by considering the ground potential deterioration, the productivity of the system with groundwater flow increased up to 80% more than that of the system without groundwater flow. This shows that for geothermal heat pump systems with high energy production, the presence of groundwater flow can improve system productivity significantly, particularly in ground with lower geothermal potential.

4.3.2 Thermo-mechanical behaviour of the pile

For analysis of the thermo-mechanical behaviour of the pile, peak days in winter and summer mode were selected. Static thermal loading and pile-soil interface sliding conditions were considered in the analysis. The heat carrier fluid temperature started from 22°C in summer mode. The only difference in this part of the analysis was inlet temperatures of 29°C and 55°C for days 15 and 30 in the

summer mode simulation. The inlet temperature was varied from 7°C to 0°C for winter mode and 0°C was set as the temperature at peak day. The results indicated that no sliding conditions occurred at the pile-soil interface. The frictional mobilised stresses at the pile-soil interface (Fig. 23) were not in range that poses a high risk of pile sliding conditions and the impact resulting from thermal operation of piles can be ignored from a design perspective. The stresses were found to be higher at the pile toe, which resulted from higher temperature variations in this region, as explained in our previous works [42,59].

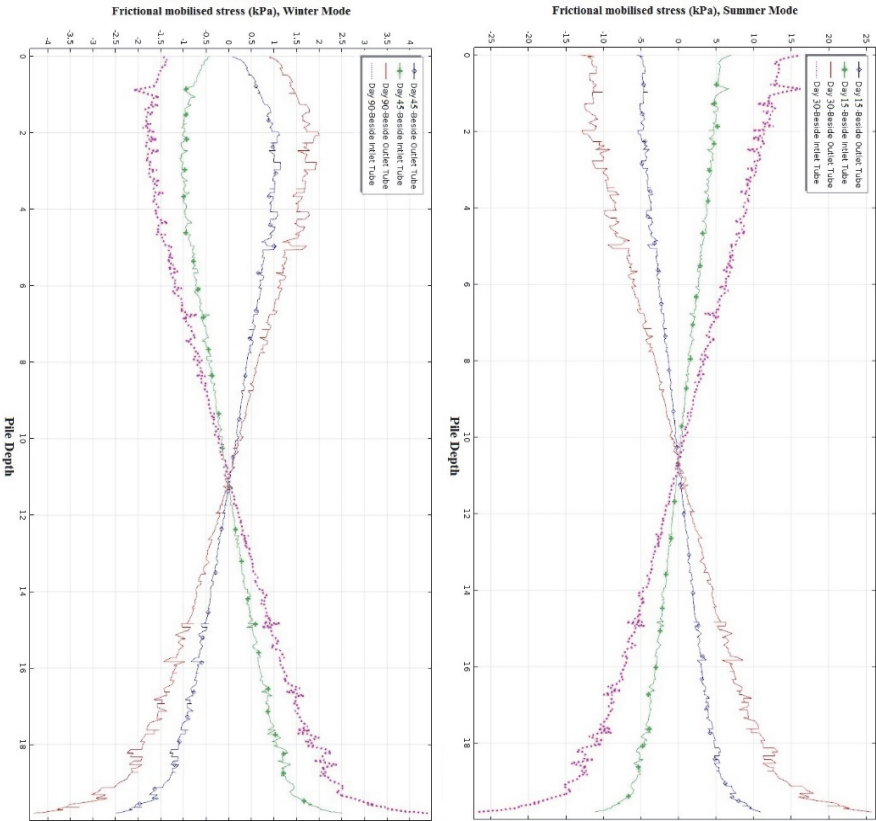


Fig. 23. Frictional mobilised stresses at the pile-soil interface under sliding contact conditions (Paper III, reprinted with permission from Journal Energy and Buildings).

Based on the axial stresses resulting from temperature variations in the pile shaft under foregoing inlet temperatures (Fig. 24), it was deduced that the stresses

generated at the pile shaft in frictional piles undergo a significantly greater decrease than the stresses in end-bearing piles [59]. These stresses were observed to be close to zero at pile head and toe. The sudden fluctuation at the pile toe in Fig. 24 indicates the thermal fluctuation around the U-tube in this region.

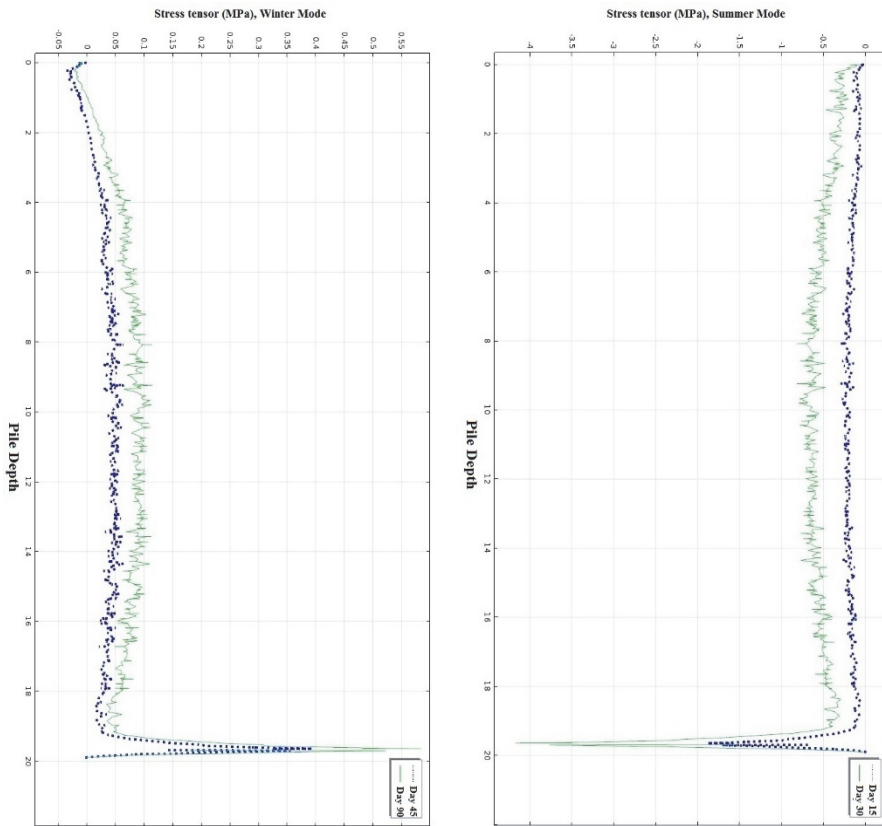


Fig. 24. Axial stresses at the centre of pile shaft under heating/cooling operations (the pile is free at head and toe) (Paper III, reprinted with permission from Journal Energy and Buildings).

Displacements of the pile shaft during different heating/cooling operations were found to range from -0.35 mm to +0.25 mm for winter mode and -1.5 mm to 2.5 mm for summer mode (Fig. 25). The null point (point without displacement) was found at a depth of -13 m. No difference was found in null point location between heating and cooling operations, indicating relatively symmetrical displacement of frictional piles in the two different operations. The value of displacements can be

considered to be negligible, but calculation of the displacements for structures sensitive to settling is still recommended.

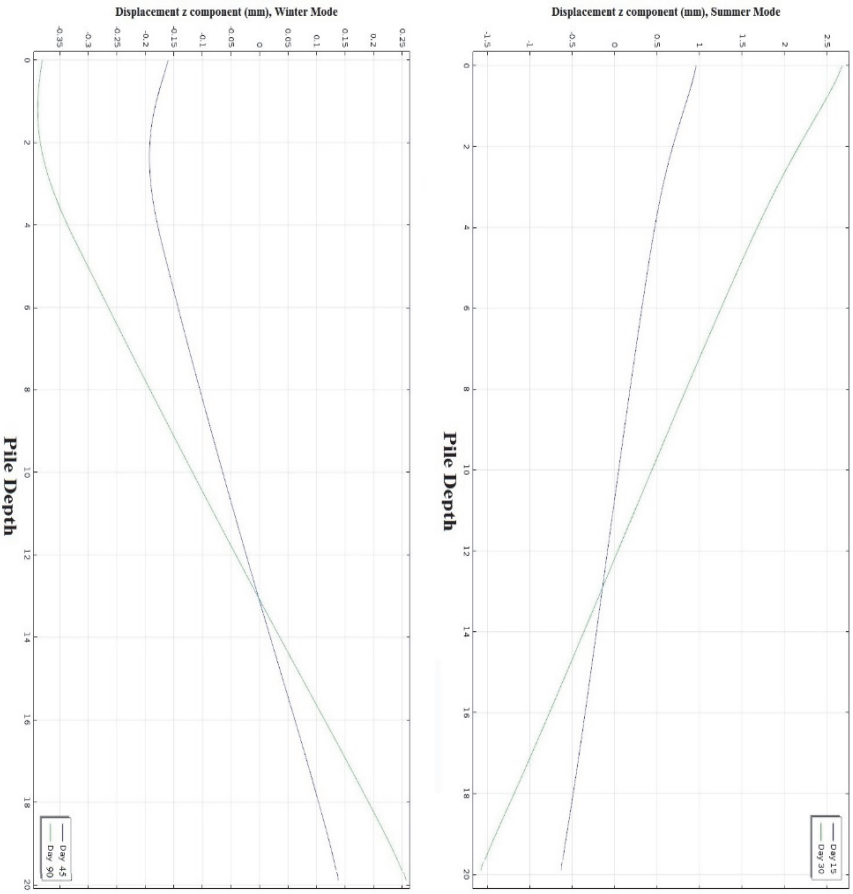


Fig. 25. Displacements at the pile shaft during heating/cooling operations (negative sign denotes upward movement and positive sign downward movement) (Paper III, reprinted with permission from Journal Energy and Buildings).

5 Conclusions and suggestions for future studies

Cost-benefit analyses of ground source heat pumps (GSHPs) to identify optimal systems must be conducted before system installation. Analysis of the thermal regime generated in the pile shaft under various system operations (heating/cooling) is essential in investigating the mechanical behaviour of the pile structure during its operating life. This study developed a numerical model for prediction of ground heat exchanger (GHE) performance with some different U-tube shapes under different fluid flow rates. Thermal regimes in the pile shaft during heating/cooling operations were also scrutinised in the horizontal and vertical axes. Based on the data obtained, the following major conclusions can be drawn:

1. In order to increase the output power of different GHEs in steel pile foundations, increasing the number of U-tubes can be more efficient than increasing the pipe diameter. For example, operating a double-tube pile with a 33% increase in fluid flow rate gave a 60% increase in output energy compared with a single-tube pile. In a single-tube and double-tube with around 28% lower fluid flow rate, around 10% more energy was obtained in the double-tube pile. For more correct prediction of the most cost-effective system, the energy produced by systems and electricity costs to provide different fluid flow circulations in closed loops must be evaluated.
2. For systems with low temperature differences between inlet fluid and ambient soil, there was no significant difference in output power. However, type of GHE can be important in achieving higher productivity if there is sufficient difference between inlet fluid and the surrounding ground temperature.
3. The thermal regime inside the pile shaft is divided into two major zones: one based on transient thermal behaviour in which the temperature profile changes over the pile length, and one steady state zone with a constant thermal profile. The transient zone dominated in the pile shaft, occurring in approximately three-quarters of the upper pile length. The average constant temperature in the steady state zone was proportionately closer to the inlet temperature when the difference between inlet temperature and average ground temperature was higher.
4. In both heating/cooling modes, there were high fluctuations in pile shaft temperature at depth below the tube curve. These fluctuations were around 1.5°C and 11°C for winter and summer mode, respectively. A temperature

fluctuation of around 15°C also occurred in the 1 m of pile length in cooling operation. Since these fluctuations occur over very short distances, calculation of the temperatures is essential in precise determination of the mechanical behaviour of energy piles.

5. Based on the thermal regimes observed here in pile shafts, assuming a constant temperature equal to inlet fluid temperature over the pile length in calculating the mechanical behaviour of energy piles can seriously impair precise prediction of the mechanical behaviour of piles. Consequently, detailed thermal analysis of the pile shaft, particularly near parallel pipes and U-curves at the pile toe where temperatures are high, is needed for this purpose.

Recent experiences have demonstrated that energy piles are sustainable and economically feasible structures if their durability (both mechanical and geotechnical) meets the requirements set by standards and design codes. Despite the large number of energy piles now being installed, use of this relatively new technology is challenging as there is a lack of reliable information concerning the thermo-mechanical behaviour of energy piles under different thermal loading conditions.

This thesis presented a three-dimensional numerical analysis of the thermo-hydro-mechanical response of a composite energy pile in heating/cooling operations, with the aim of developing a reliable numerical model to analyse pile behaviour and to investigate the thermal stresses, deformations and shaft friction during heating/cooling. The pile was assumed to be supported on a stiff soil layer at its toe and attached by a fixed connection to the superstructure (pile cap). The simulation results were compared with experimental test results (Lausanne) and a good correlation was found. Based on the simulation results, the following major conclusions were drawn:

1. The maximum stresses in concrete during heating and cooling operations occurred in the vicinity of downward and upward ground heat exchanger tubes, respectively. The calculated maximum tensile and compressive stresses during contraction and expansion (inlet temperature 27°C) were around +0.6 MPa and -5.7 MPa, respectively. The tensile stresses were small in comparison with stresses due to the dead and live loads of the building. At a rough estimate, the thermal compressive stresses at an inlet temperature of 27°C in expansion mode were about 20% of the ultimate compressive strength of typical concrete (30 MPa). This indicates that in a design context, the structural bearing capacity of piles needs to be reduced significantly due to the additional thermal

stresses. Stresses in the steel shaft of the pile were also found to be negligible in comparison with the high ultimate yield strength of steel.

2. In end-bearing piles during contraction, with a reduction in fluid flow temperature, the null point was found to move upward, while during expansion no tangible variation in null point location was observed. Furthermore, during contraction the maximum displacement occurred at the pile toe and amounted to 0.7 mm with an inlet fluid temperature of 0°C. The maximum displacement during expansion was around 0.26 mm and displacement decreased over the simulation with increasing pile temperature.
3. Pile expansion/contraction during heating/cooling operations affected the pile-soil interaction. The maximum mobilised shaft friction (15 kPa) occurred during contraction, while friction values during expansion were insignificant. The variations in shaft friction were more critical for frictional (cohesion) piles than for end-bearing piles.

It is very important that the output power of GSHPs be calculated and optimised before system installation. Pile foundations coupled with GSHPs are sustainable and economically feasible structures if their structural and geotechnical capacities remain within the values recommended by standards and design codes. In this study, a frictional energy pile foundation was simulated using finite element analysis on real operating conditions of an energy pile, emulating GHE performance in service mode. Two different groundwater conditions were considered in the analysis; soil with groundwater flow and soil without groundwater flow. The thermo-mechanical behaviour of a pile was also evaluated by considering static thermal loading and possible sliding conditions at the pile-soil interface. Based on the simulation results, it was concluded that:

- For systems with low geothermal potential in absorbing/injecting heat, differences between systems with and without groundwater flow are more significant. When only one tube with low energy transfer capacity is installed in the pile, there is always sufficient geothermal potential in the soil in the vicinity of the pile and groundwater flow will not increase the potential significantly. When higher transfer capacity is installed, the heat absorption may decrease the ground temperature in the vicinity of the pile. In such conditions, groundwater flow can transfer heat from surrounding areas and thereby increase the ground temperature and the geothermal potential near the pile. According to the numerical analysis in this thesis, in the latter case the groundwater flow can increase the productivity of the system by at least 20%

in winter mode. The increase in summer mode productivity was at maximum 5%, owing to higher ground potential for heat absorption.

- Systems with high heat injection into the ground during summer (using solar panels etc.) in order to increase the ground's potential as a heat source in winter are not recommended under groundwater flow conditions, due to heat energy dissemination resulting from flow effects.
- No sliding occurs at the pile-soil interface and the frictional stresses at the pile-soil interface are not in the high risk range for pile sliding. Therefore the effects of sliding conditions resulting from pile thermal performance can be overlooked from a design perspective. These stresses were higher at the pile toe as a result of higher temperature variations in this region.
- The thermal axial stresses generated in frictional pile shafts are less than the thermal stresses in end-bearing pile shafts. These stresses are negligible at pile head and toe. A sharp fluctuation was identified at the pile toe resulting from thermal fluctuations at the pile shaft around the U-curve at this region.
- Pile displacements are within the range -0.35 mm to +0.25 mm for winter mode and -1.5 mm to 2.5 mm for summer mode. The null point (point without displacement) is located at a depth of around -13 m. No change in location of the null point in different operating modes and under different thermal loadings was seen for a frictional pile with freely supported head and toe. The value of displacements was nearly negligible, but calculation of displacements for structures sensitive to settling is recommended.

Future studies

In future studies, more investigations should be carried out on the thermo-mechanical behaviour of different thermo-active structures, such as tunnels etc. Further investigations can be directed at interactions between thermo-active geostructures and structures like those between pile cap and raft foundations or between bridge piers and bridge superstructures, which can be influenced by deformations of piers under different thermal loadings.

In future, more investigations should be carried out on temperature-induced stresses in piles under different degrees of fixed support at the pile cap caused by the rigidity of raft foundations or structures over the foundation, which can influence the range of these stresses. For structures sensitive to settling, more research can be carried out based on variations in soil thermal properties under different thermal conditions which can induce future settling and also different pile-

soil interface properties in soils sensitive to temperature variations. For energy efficiency, the long-term feasibility of energy piles for use for around 50 years should be determined, as it can be of great importance for cost-effective construction of these systems compared with the fairly high initial investment in system installation.

List of references

1. Snäkin JPA (2000) An engineering model for heating and emission assessment the case of North Karelia Finland. *Applied Thermal Energy* 67 (4): 353–381.
2. Ministry of the Environment, Finland (2011) Finland is implementing the Kyoto Protocol. URL: <http://www.ymp.fi/en-US>.
3. Statistics Finland, Energy Statistics (2013) URL: <http://tilastokeskus.fi/>. Cited 2013/05/06.
4. Christopher JW, Hao L & Saffa BR (2010) An investigation of the heat pump performance and ground temperature of a piled foundation heat exchanger system for a residential building. *Energy* 35 (12): 4932–4940.
5. Gao J, Zhang X, Liu J, Shan li K & Yang J (2008) Thermal performance and ground temperature of vertical pile-foundation heat exchangers: a case study. *Appl. Therm. Eng.* 28 (17–18): 2295–2304.
6. Bloomquist RG (2003) Geothermal space heating. *Geothermics* 32 (4–6) 513–526.
7. Ozgener L, Hepbasli A & Dincer I (2006) Performance investigation of two geothermal district heating systems for building applications: energy analysis. *Energy Build.* 38 (4): 286–292.
8. Yang WB, Shi MH & Dong H (2006) Numerical simulation of the performance of a solar–earth source heat pump system. *Appl. Therm. Eng.* 26 (17–18): 2367–2376.
9. Ozgener L, Hepbasli A & Dincer I (2007) A key review on performance improvement aspects of geothermal district heating systems and applications. *Renewable Sustainable Energy Rev.* 11 (8): 1675–1697.
10. Hepbasli A (2003) Current status of geothermal energy applications in Turkey. *Energy Sources* 25 (7): 667–677.
11. Nairen D, Qinyun L & Zhaohong F (2004) Heat transfer in ground heat exchangers with groundwater advection. *Int. J. Therm. Sci.* 43: 1203–1211.
12. Fan R, Jiang Y, Yao Y, Shiming D & Ma Z (2007) A study on the performance of a geothermal heat exchanger under coupled heat conduction and groundwater advection. *Energy* 32 (11): 2199–2209.
13. Laloui L, Nuth M & Vulliet L (2006) Experimental and numerical investigations of the behaviour of a heat exchanger pile. *Int. J. Numer. Anal. Methods Geomech.* 30: 763–781.
14. Quick H, Meissner S & Michael J (2005) Innovative foundation systems for high-rise buildings, First Intelligent Building Middle East Conference.
15. Pahud D, Hubbuch M (2007) Measured thermal performances of the energy pile system of the dock midfield at Zurich Airport. *Eur. Geotherm. Cong.*
16. Adam D & Markiewicz R (2009) Energy from earth-coupled structures: foundations, tunnels and sewers. *Geotechnique* 59 (3): 229–236.
17. Carslaw HS & Jaeger JC (1946) *Conduction of Heat in Solids*. Clarendon Press, Oxford.
18. Mei VC & Emerson CJ (1985) New approach for analysis of ground-coil design for applied heat pump systems. *ASHRAE Transactions* 91 (2B): 1216–1224.

19. Deerman JD & Kavanaugh SP (1991) Simulation of vertical U-tube ground coupled heat pump systems using the cylindrical heat source solution. *ASHRAE Transactions* 97 (1): 287–295.
20. Yavuzturk C, Spitler JD & Rees SJ (1999) A transient two-dimensional finite volume model for the simulation of vertical U-tube ground heat exchangers. *ASHRAE Transactions* 105 (2): 465–474.
21. Ochifuji K & Kim NC (1988) Theoretical analysis of heat conduction of long term heat storage and extraction by buried vertical pipe system. *Transactions of the Society of Heating, Air-Conditioning and Sanitary Engineers of Japan* 36: 1–9.
22. Bernier M (2001) Ground-coupled heat pump system simulation. *ASHRAE Transactions* 106 (1): 605–616.
23. Den Braven K & Nilson E (1998) Performance prediction of a sub-slab heat exchanger for geothermal heat pumps. *Journal of Solar Energy Engineering* 120 (4): 282–288.
24. Gauthier C, Lacroix M & Bernier H (1997) Numerical simulation of soil exchanger-storage systems for greenhouses. *Solar Energy* 60: 333–346.
25. Li X, Chen Y, Chen Z & Zhao J (2006) Thermal performances of different types of underground heat exchangers. *Energy Build* 38 (5): 543–7.
26. Ozgener O, Hepbasli A (2007) Modeling and performance evaluation of ground source (geothermal) heat pump systems. *Energy and Buildings* 39 (1): 66–75.
27. Esen H, Inalli M & Esen M (2007) Numerical and experimental analysis of a horizontal ground-coupled heat pump system. *Building and Environment* 42 (3): 1126–1134.
28. Nam Y, Ooka R & Hwanga S (2008) Development of a numerical model to predict heat exchange rates for a ground-source heat pump system. *Energy and Buildings* 40 (12): 2133–2140.
29. De Moel M, Bach PM, Bouazza A, Singh RM & Sun JO (2010) Technological advances and applications of geothermal energy pile foundations and their feasibility in Australia. *Renewable and Sustainable Energy Reviews* 14: 2683–2696.
30. Brandl H (2006) Energy foundations and other thermo-active ground structures. *Geotechnique* 56 (2): 81–122.
31. Suryatriyastuti ME, Mroueh H & Burlon S (2012) Understanding the temperature induced mechanical behaviour of energy pile foundations. *Renew Sustain Energy Rev* 16: 3344–54.
32. Comsol Multiphysics (2013) Finite element analysis and engineering simulation software (Version 4.3b).
33. Zanchini E, Lazzari S & Priarone A (2012) Long-term performance of large borehole heat exchanger fields with unbalanced seasonal loads and groundwater flow. *Energy* 38 (1): 66–77.
34. Comsol Multiphysics (2013) Finite element analysis and engineering simulation software (Version 4.3a). User's Guide, Heat Transfer Module, Chapters 2&7: Conjugate Heat transfer Branch.
35. Leong WH, Tarnawski VR & Aittomaki A (1998) Effect of soil type and moisture content on ground heat pump performance, *International Journal of Refrigeration* 21 (8): 595–606.

36. Adam D & Markiewicz R (2009) Energy from earth-coupled structures, foundations, tunnels and sewers. *Geotechnique* 59 (3): 229–236.
37. Gao J, Zhang X, Liu J, Shan Li K & Yang J (2008) Thermal performance and ground temperature of vertical pile-foundation heat exchangers: a case study. *Applied Thermal Engineering* 28 (17–18): 2295–2304.
38. Comsol Multiphysics (2013) Finite element analysis and engineering simulation software (Version 4.3a). Software material library.
39. Adam D, Markiewicz R & Der N (2003) Geothermischen Energie mittels erdberührter Bauwerke. *Österreichische Ingenieur-und Architekten-Zeitschrift* 148 (1): 2–12.
40. Rawlings RHD & Sykulski JR (1999) Ground source heat pumps: a technology review. *Building Service Engineering Research and Technology* 20 (3): 119–129.
41. Wang H & Qi C (2008) Performance study of underground thermal storage in a solar-ground coupled heat pump system for residential buildings, *Energy and Buildings* 40 (7): 1278–1286.
42. Gashti EHN, Uotinen VM & Kujala K (2014) Numerical modelling of thermal regimes in steel energy pile foundations: a case study. *Energy Build* 69: 165–74.
43. Comsol Multiphysics (2013) Finite element analysis and engineering simulation software (Version 4.3b). User's guide, Structural mechanics module: theory for the solid mechanics user interface [Chapter 3].
44. Amatya BL, Soga K, Bourne-Webb PJ, Amis T & Laloui L (2012) Thermo-mechanical behaviour of energy piles. *Geotechnique* 62 (6): 503–19.
45. Adkins CJ (1983) *Equilibrium thermodynamics*. Cambridge University Press.
46. Yourgrau W, Van Der Merwe A & Raw G (2002) *Treatise on irreversible and statistical thermodynamics: an introduction to nonclassical thermodynamics*. Dover.
47. Lubarda VA (2004) On thermodynamic potentials in linear thermoelasticity. *Int J Solids Struct* 41(26): 7377–98.
48. Duwel A, Candler RN, Kenny TW & Varghese M (2006) Engineering MEMS resonators with low thermoelastic damping. *J Microelectromech Syst* 15 (6): 1437–45.
49. Gurtin ME, Fied E & Anand L (2010) *The mechanics and thermodynamics of continua*. In: Cambridge, Academic Press.
50. Ground Source Heat Pump Association (2012) *Thermal pile; design, installation & materials standards*. Knowlhill: United Kingdom. Design & Installation: Personnel & Training Requirements Chapter.
51. Loveridge FA, Smith P & Powrie W (2013) *A review of design and construction aspects for bored thermal piles*. Ground engineering. University of Southampton.
52. Laloui L (2001) Thermo-mechanical behaviour of soils. *Revue Francaise de genie Civil* 5(6): 809–43.
53. Cekerevac C & Laloui L (2004) Experimental study of thermal effect of the mechanical behaviour of a clay. *Int J Numer Anal Meth Geomech* 28: 209–228.
54. Mroueh H & Shahroui I (2009) Numerical analysis of the response of battered piles to inclined pullout loads. *Int J Numer Anal Meth Geomech* 33(10): 1277–1288.
55. De Gennaro V, Frank R (2005) Modelisation de l'interaction sol-pieu par la méthode des elements finis. *Bull Lab Ponts Chaussees RÉF 4552*: 107–133.

56. Bourne Webb PJ, Amatya B, Soga K, Amis T, Davidson C & Payne P (2009) Energy pile test at Lambeth College, London: geotechnical and thermodynamic aspects of pile response to heat cycles. *Geotechnique* 59 (3): 237–248.
57. Geotechdata.info, Angle of friction (2013) Soil friction angle is a shear strength parameter of soils. URI: <http://www.geotechdata.info/parameter/angle-of-friction.html>.
58. Swiss Standard SN-670010 (2011) Association of Swiss Road and Traffic Engineers. Characteristic coefficients of soils. *Geotechnische Erkundung und Untersuchung, Geotechnische Kenngrößen*.
59. Gashti EHN, Malaska M & Kujala K (2014) Evaluation of thermo-mechanical behaviour of composite energy piles during heating/cooling operations. *Eng. Struct.* 75 363–373.
60. Nield D & Bejan A (2006) *Convection in Porous Media*. third ed., Springer, New York.
61. Bars ML & Worster MG (2006) Interfacial Conditions Between a Pure Fluid and a Porous Medium: Implications for Binary Alloy Solidification. *J. Fluid Mech.* 550: 149–173.
62. Hamdhan IN & Barry GC (2010) Determination of thermal conductivity of coarse and fine sand soils, in: *Proceedings World Geothermal Congress, Indonesia*.
63. Freeze RA & Cherry JA (1979) *Groundwater*. Prentice-Hall, Inc, Englewood Cliffs, N.J. pp. 604.
64. Rybach L & Eugster WJ (2002) Sustainability aspects of geothermal heat pumps, In: *27th workshop on geothermal reservoir engineering, California*.
65. Rybach L, Megel T & Eugster WJ (2000) At what time scale are geothermal resources renewable? In: *World geothermal congress, Japan*.
66. Signorelli S, Kohl T & Rybach L (2005) Sustainability of production from borehole heat exchanger fields, In: *World geothermal congress, Turkey*.
67. Bourne-Webb PJ, Amatya B & Soga K (2013) A framework for understanding energy pile behaviour. *Proc Inst Civ Eng-Geotech Eng* 2013; 166: 170 –7. ISSN 1353-2618.

Original publications

- I Hassani Nezhad Gashti E, Uotinen V-M, Kujala K, (2014) Numerical modelling of thermal regimes in steel energy pile foundations: A case study. *Energy and Buildings* 69: 165-174.
- II Hassani Nezhad Gashti E, Malaska M, Kujala K, (2014) Evaluation of thermo-mechanical behaviour of composite energy piles during heating/cooling operations. *Engineering Structures* 75: 363-373.
- III Hassani Nezhad Gashti E, Malaska M, Kujala K, (2015) Analysis of thermos-active pile structures and their performance under groundwater flow conditions. *Energy and Buildings* 105: 1–8.

Reprinted with permission from Elsevier: Papers (I), (II) and (III).

Original publications are not included in the electronic version of the thesis.

579. Kinnunen, Tuomo (2016) Product management perspectives on stakeholder and business opportunity analyses in the front-end of product creation
580. Heiderscheidt, Elisangela (2016) Evaluation and optimisation of chemical treatment for non-point source pollution control : purification of peat extraction runoff water
581. Su, Xiang (2016) Lightweight data and knowledge exchange for pervasive environments
582. Kaijalainen, Antti (2016) Effect of microstructure on the mechanical properties and bendability of direct-quenched ultrahigh-strength steels
583. Lanz, Brigitte (2016) Compact current pulse-pumped GaAs–AlGaAs laser diode structures for generating high peak-power (1–50 watt) picosecond-range single optical pulses
584. Kähäri, Hanna (2016) A room-temperature fabrication method for microwave dielectric Li₂MoO₄ ceramics and their applicability for antennas
585. Chowdhury, Helal (2016) Data download on the move in visible light communications: design and analysis
586. Kekäläinen, Kaarina (2016) Microfibrillation of pulp fibres : the effects of compression-shearing, oxidation and thermal drying
587. Raatikainen, Mika (2016) Intelligent knowledge discovery on building energy and indoor climate data
588. Varjo, Sami (2016) A direct microlens array imaging system for microscopy
589. Haapakangas, Juho (2016) Coke properties in simulated blast furnace conditions : Investigation on hot strength, chemical reactivity and reaction mechanism
590. Erkkilä-Häkkinen, Sirpa (2016) Rakentamisen työturvallisuuteen suhtautuminen toimijoiden kokemuksina
591. Hassani Nezhad Gashti, Ehsan (2016) Thermo-mechanical behaviour of ground-source thermo-active structures
592. Sulasalmi, Petri (2016) Modelling of slag emulsification and slag reduction in CAS-OB process
593. Liyanage, Madhusanka (2016) Enhancing security and scalability of Virtual Private LAN Services

S E R I E S E D I T O R S

A
SCIENTIAE RERUM NATURALIUM

Professor Esa Hohtola

B
HUMANIORA

University Lecturer Santeri Palviainen

C
TECHNICA

Postdoctoral research fellow Sanna Taskila

D
MEDICA

Professor Olli Vuolteenaho

E
SCIENTIAE RERUM SOCIALIUM

University Lecturer Veli-Matti Ulvinen

E
SCRIPTA ACADEMICA

Director Sinikka Eskelinen

G
OECONOMICA

Professor Jari Juga

H
ARCHITECTONICA

University Lecturer Anu Soikkeli

EDITOR IN CHIEF

Professor Olli Vuolteenaho

PUBLICATIONS EDITOR

Publications Editor Kirsti Nurkkala

ISBN 978-952-62-1405-4 (Paperback)

ISBN 978-952-62-1406-1 (PDF)

ISSN 0355-3213 (Print)

ISSN 1796-2226 (Online)

